Stem Cell Reports
Article

ISSCR

OPEN ACCESS

Recapitulation of Extracellular LAMININ Environment Maintains Stemness of Satellite Cells *In Vitro*

Kana Ishii,[1] Hidetoshi Sakurai,[2] Nobuharu Suzuki,[1] Yo Mabuchi,[1] Ichiro Sekiya,[3] Kiyotoshi Sekiguchi,[4] and Chihiro Akazawa[1,*]

[1]Department of Biochemistry and Biophysics, Graduate School of Health Care Sciences, Tokyo Medical and Dental University (TMDU), 1-5-45 Yushima, Building 3, Bunkyo-ku, Tokyo 113-8510, Japan
[2]Center for iPS Cell Research and Application (CiRA), Kyoto University, Sakyo-ku, Kyoto 606-8507, Japan
[3]Center for Stem Cell and Regenerative Medicine, Tokyo Medical and Dental University, Bunkyo-ku, Tokyo 113-8510, Japan
[4]Division of Matrixome Research and Application, Institute for Protein Research, Osaka University, Suita, Osaka 565-0871, Japan
*Correspondence: c.akazawa.bb@tmd.ac.jp
https://doi.org/10.1016/j.stemcr.2017.12.013

SUMMARY

Satellite cells function as precursor cells in mature skeletal muscle homeostasis and regeneration. In healthy tissue, these cells are maintained in a state of quiescence by a microenvironment formed by myofibers and basement membrane in which LAMININs (LMs) form a major component. In the present study, we evaluated the satellite cell microenvironment *in vivo* and found that these cells are encapsulated by LMα2–5. We sought to recapitulate this satellite cell niche *in vitro* by culturing satellite cells in the presence of recombinant LM-E8 fragments. We show that treatment with LM-E8 promotes proliferation of satellite cells in an undifferentiated state, through reduced phosphorylation of JNK and p38. On transplantation into injured muscle tissue, satellite cells cultured with LM-E8 promoted the regeneration of skeletal muscle. These findings represent an efficient method of culturing satellite cells for use in transplantation through the recapitulation of the satellite cell niche using recombinant LM-E8 fragments.

INTRODUCTION

Regeneration of adult skeletal muscle regeneration is mediated by tissue-specific muscle stem cells, also known as satellite cells (Mauro, 1961). Satellite cells reside in a specialized niche environment situated between the basement membrane of the muscle tissue and the plasma membrane of constituent myofibers (Relaix and Zammit, 2012). This niche structurally orients satellite cell mitosis (Kuang et al., 2008). In adult skeletal muscle, satellite cells are maintained in a state of quiescence until tissue damage or other stimuli cause these cells to become activated, proliferate, and subsequently differentiate into mature myofibers (Charge and Rudnicki, 2004). A small number of activated satellite cells self-renews and returns to the quiescent state maintaining a reservoir of stem cells for homeostasis and repair (Olguin and Olwin, 2004; Zammit et al., 2004). The paired box transcription factor PAX7 is critical for maintaining satellite cell function (von Maltzahn et al., 2013) and, together with the myogenic regulator, MYOD, is a key determinant of satellite cell fate (Zammit et al., 2002). Satellite cell behavior is regulated by multiple signaling pathways such as MAPK protein, c-Jun N-terminal kinase (JNK), and p38 MAPK (Alter et al., 2008; Bernet et al., 2014; Charville et al., 2015; Cosgrove et al., 2014; Troy et al., 2012).

PAX7-expressing cells are necessary and sufficient for muscle regeneration (Lepper et al., 2011; Sambasivan et al., 2011). Transplantation of autologous satellite cells modified to express DYSTROPHIN is being studied as a potential therapeutic approach in Duchenne muscular dystrophy (DMD) (Ikemoto et al., 2007). However, satellite cells begin to differentiate immediately upon losing contact with their niche environment; in culture, satellite cells cease to express PAX7 and lose their capacity to support regeneration (Montarras et al., 2005). Efficient techniques for expanding satellite cells in an undifferentiated state *in vitro* are thus urgently needed. Previous studies have reported the culture of undifferentiated satellite cells by manipulation of NOTCH signaling (Parker et al., 2012), substrate elasticity (Gilbert et al., 2010), or regulation of p38 activation (Bernet et al., 2014; Charville et al., 2015; Cosgrove et al., 2014). We therefore sought to identify efficient methods of mimicking the satellite cell niche to enable more efficient expansion of satellite cells *in vitro*.

Components of the cellular microenvironment, such as ECM, play essential roles in the maintenance of satellite cell stemness (Dumont et al., 2015; Thomas et al., 2015). Changes in the composition of ECM during muscle development and regeneration affect quiescence, activation, differentiation, and self-renewal in satellite cells. During muscle regeneration, the expression of ECM proteins, including COLLAGEN, FIBRONECTIN, and LAMININ (LM), is induced in skeletal muscle and required for the maintenance of satellite cells (Bentzinger et al., 2013; Disatnik and Rando, 1999; Johansson et al., 1997; Urciuolo et al., 2013). However, much remains to be learned about the architecture and structural components of ECM in regard of satellite cell microenvironment and the signals that these factors provide to maintain satellite cells in a

quiescent state. LMs, a glycoprotein family with a cross-shaped structure, consisting of α, β, and γ chains, constitute a major component of the ECM in the skeletal muscle basement membrane (Miner and Yurchenco, 2004). The α chain is expressed in a tissue- and developmental stage-specific manner, and mouse knockout models for each α chain variant exhibit different phenotypes (Guo et al., 2003; Heng et al., 2011). In skeletal muscle, LMα2 is specifically localized in the basement membranes (Yao et al., 1996). Loss of the LMα2 subunit leads to progressive muscular dystrophy and has been used as a model of congenital muscular dystrophy (Helbling-Leclerc et al., 1995). LMα4 and α5 are expressed in embryonic muscle basal lamina, and LMα5 is expressed in adult muscle during regeneration in cardiotoxin mouse muscle injury models and in DMD tissue (Patton et al., 1999). LMs function in cell-to-basement membrane adhesion (Domogatskaya et al., 2012). Signaling from LM to cells via INTEGRIN regulates cell survival and differentiation (Disatnik and Rando, 1999). Satellite cells can be cultured on a variety of ECM substrates including Matrigel, GELATIN, COLLAGEN, and LM111 (Danoviz and Yablonka-Reuveni, 2012; Grefte et al., 2012; Zou et al., 2014). Although LM is commonly used for satellite cell culture, the expression of LMs as components of the structural microenvironment of satellite cells has not been elucidated.

In the present study, we show that the LMα3, α4, and α5 chains, together with LMα2 in the basement membrane, are components of the satellite cell niche in skeletal muscle tissue in both mouse and human. In an effort to functionally replicate the extracellular LM environment of satellite cells *in vitro*, we prepared recombinant LM-E8 fragments, which consist of the C-terminal half of the coiled-coil region of the LM protein with the LM globular domains 1–3. LM-E8 fragments exhibit INTEGRIN-binding activity equivalent to that of intact LMs (Miyazaki et al., 2012). We show that reconstitution of extracellular LM environment by LM-E8 maintains satellite cells in an undifferentiated state through regulation of JNK and p38 signaling. These findings show that satellite cells can be maintained and expanded *ex vivo* through the functionally replication of the human/mouse satellite cell niche environment with LM-E8 fragments and that satellite cells cultured under these conditions retain their ability to contribute to muscle regeneration.

RESULTS

LM α3, α4, and α5 Are Extracellular Components of Satellite Cells

LMs are the major component of the satellite cell niche and function in cell-to-basement membrane adhesion (Domogatskaya et al., 2012). We analyzed the expression pattern of each LM α chain in mouse skeletal muscle. Tibialis anterior (TA) muscles were stained with antibodies for each LM α chain and PAX7, a marker of satellite cells. We found that $PAX7^+$ quiescent satellite cells were surrounded by LMα3, α4, and α5 (Figures 1A and 1B). In addition, LMα4 and α5 were detected in blood vessel basement membrane. We did not detect the expression of LMα1 in skeletal muscle. Consistent with reports from previous studies, the basement membranes of mature muscle fibers were stained with LMα2 (Helbling-Leclerc et al., 1995; Holmberg and Durbeej, 2013).

To examine the expression of LMs in self-renewing satellite cells, we next analyzed regenerating TA muscle tissue. Muscle regeneration was induced by cardiotoxin. Interestingly, we found that the expression of LMα3, α4, and α5 was closely associated with $PAX7^+KI67^-$ self-renewed satellite cells, which were located at the edges of regenerating muscle fibers (Figures 1C and S1A–S1C). Sequential scanning images showed that self-renewed satellite cells are encapsulated by a pericellular matrix composed of LMα3, α4, and α5 (Figure 1C). In contrast, the expression of LMα3, α4, and α5 chains, particularly that of the α4 and α5 chains, adjacent to $PAX7^+KI67^+$-activated satellite cells, seemed to be reduced in the regenerating tissue (Figures S1D–S1F, left). These results indicate that satellite cells, especially those that have undergone self-renewal, are encapsulated in LMα3, α4, and α5 chains.

Reconstitution of Extracellular LM Environment by LM-E8 Fragments

Our expression analyses of LM α subunits led us to speculate that components of extracellular LM isoforms might play roles in maintaining PAX7 expression in cultured satellite cells. We prepared recombinant LM-E8 fragments, which are minimally active fragments of LMs retaining the INTEGRIN-binding sites (Figure 2A). Quiescent satellite cells were directly isolated from 8-week-old mouse muscle by fluorescence-activated cell sorting (FACS) using the SM/C-2.6 antibody, which recognizes an antigen expressed in satellite cells (Figure S2) (Fukada et al., 2004). To reconstitute the extracellular/pericellular LM environment, we tested different culture conditions using the LM-E8 fragments: culture on LM111-E8; culture on LM211-E8; culture on LM322-, 411-, and 511-E8; pretreatment with LM332-, 411-, and 511-E8, and then culture on Matrigel; pretreatment with LM332-, 411-, and 511-E8, and then culture on LM211-E8; we termed this last condition "Pre3/4/5-on2" (Figure 2B). We also tested several other different culture conditions using the LM-E8 fragments (Figure S3). Culture on Matrigel without pretreatment was used as a control (Danoviz and Yablonka-Reuveni, 2012; Motohashi et al., 2014), as Matrigel containing LM111 is the most common substrate that stabilizes the expression of PAX7 when culturing satellite cells, more so than gelatin and

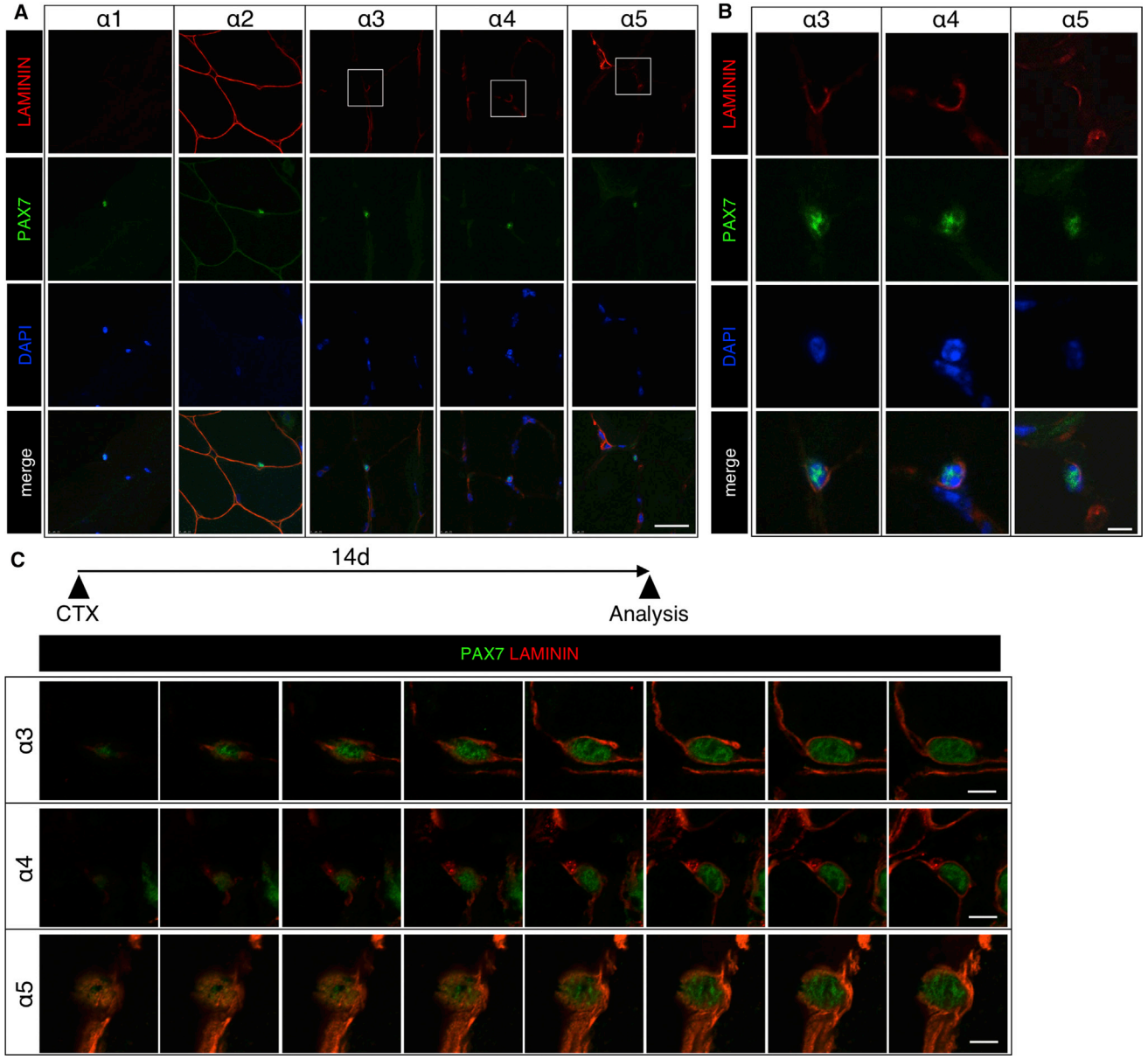

Figure 1. Expression of LM α Chains in Mouse Skeletal Muscle

(A) LM immunofluorescence using anti-α1, α2, α3, α4, and α5 chain antibodies is shown in red. PAX7 was used as a satellite cell maker (green) and DAPI was used a nuclear maker (blue). Scale bar represents 20 μm.

(B) High-magnification view of LMα3, α4, and α5 expression around satellite cells. Scale bar represents 5 μm.

(C) High-magnification view of LMα3, α4, and α5 expression around satellite cells 14 days after cardiotoxin (CTX) injection (sequential scanning image). Muscle tissue was stained with anti-LMα3-5 antibody (red) and anti-PAX7 antibody (green) in satellite cells. Scale bar represents 5 μm.

collagen (Danoviz and Yablonka-Reuveni, 2012; Grefte et al., 2012). We also observed that sorted satellite cells barely attached and proliferated scarcely on a gelatin-coated dish (data not shown). We found that the relative fluorescence intensity of PAX7 was highest in the Pre3/4/5-on2 group (Figure 2C). We detected LM332-, 411-, and 511-E8 fragments around isolated satellite cells after pre-treatment (Figure 2D). Because E8 fragments were detected with the HA tag attached to the β chain, it remains unclear whether all of the LM332-, 411-, and 511-E8 fragments were deposited around satellite cells. These data suggest that functional reconstitution of the extracellular LM

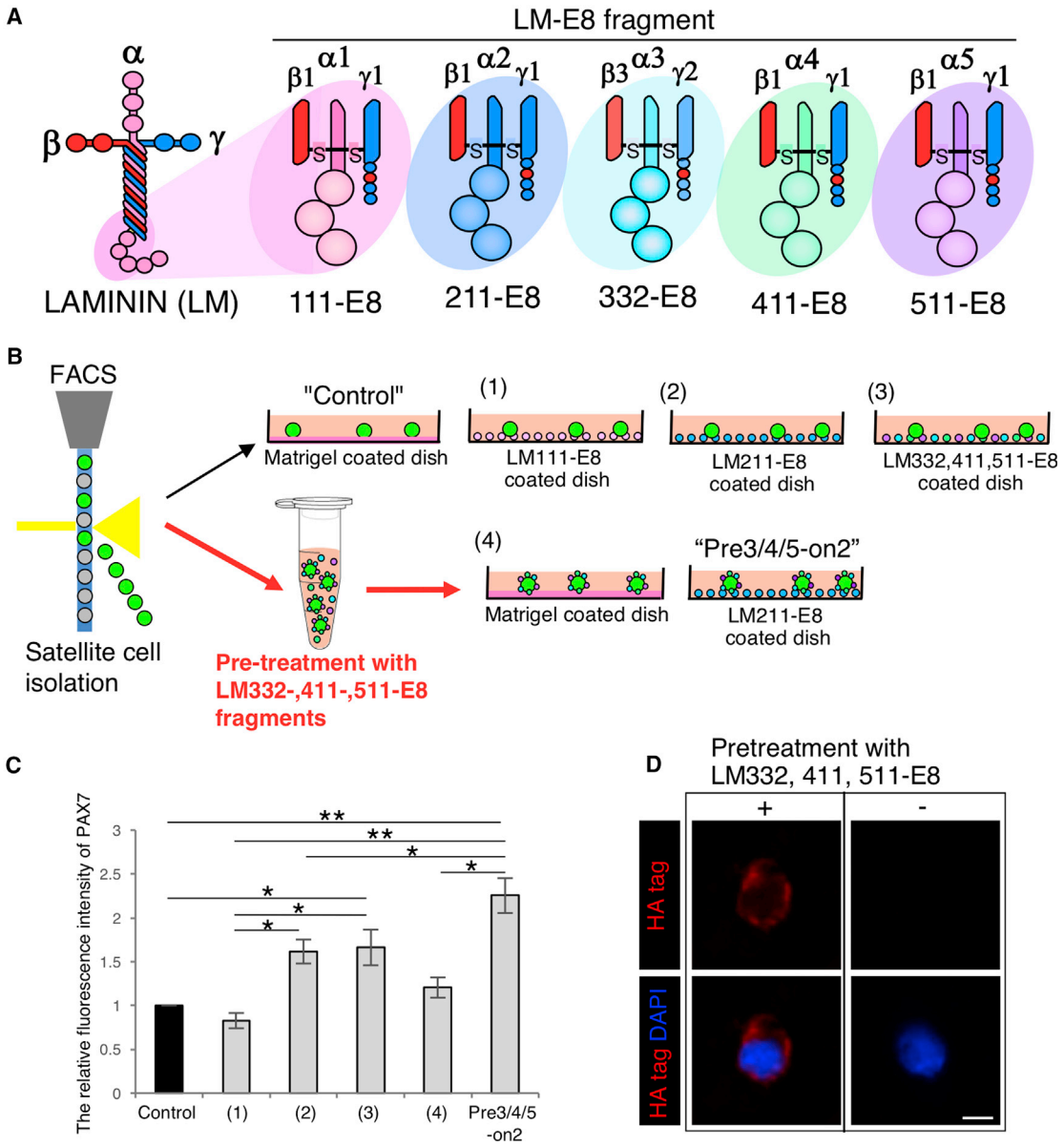

Figure 2. Reconstitution of Extracellular LM Environment by LM-E8

(A) Schematic of LM 111-, 211-, 332-, 411-, and 511-E8 fragments.

(B) Culture method used for isolated satellite cells.

(C) The relative fluorescence intensity of PAX7 after 5 days in culture on the Matrigel control or the combination of LM-E8 fragments. The ratio of the Matrigel control was set as 1.0. n = 3 independent experiments. Error bars, SEM; *p < 0.05, **p < 0.01.

(D) Immunostaining for HA tag (red) and DAPI (blue) of cells treated by LM 332-, 411-, and 511-E8. Scale bar represents 5 μm.

environment using LM-E8 can maintain undifferentiated satellite cells expressing PAX7 *in vitro*.

Reconstitution of Extracellular LM Environment Maintains Satellite Cells in an Undifferentiated State while Retaining Their Proliferative Capacity

PAX7 is expressed in both quiescent and activated satellite cells, and is downregulated when satellite cells commit to differentiation (Kuang and Rudnicki, 2008; Sambasivan and Tajbakhsh, 2007; Tedesco et al., 2010). To investigate whether differentiation of satellite cells is suppressed in the Pre3/4/5-on2 condition, we labeled satellite cells with PAX7 and MYOD to distinguish them from committed myogenic cells (Figure 3A). We observed that the immunofluorescence level of PAX7 was higher in the Pre3/4/5-on2 group than in the Matrigel control (Figure 3B). We also

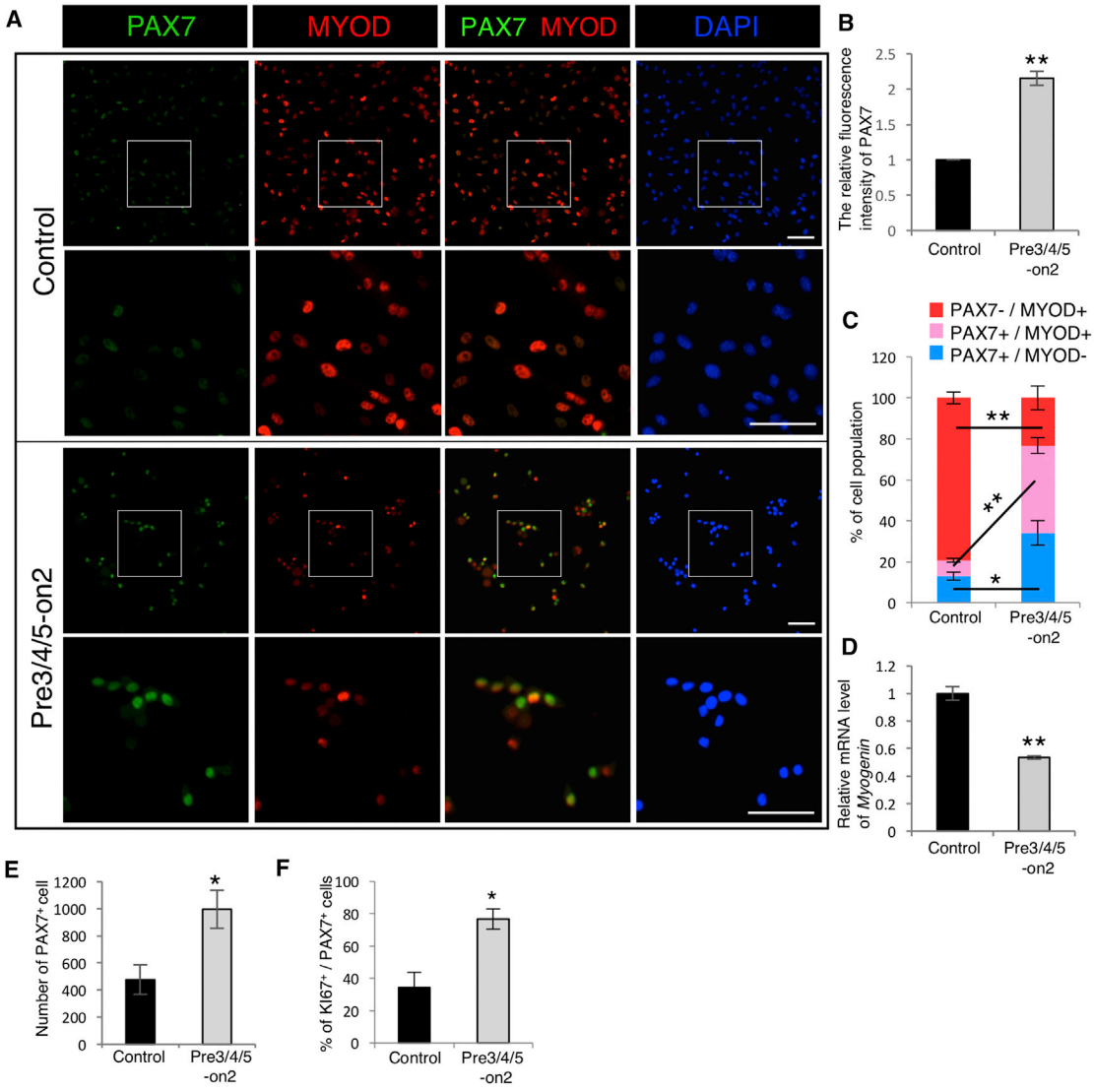

Figure 3. LM-E8 Fragments Maintain Undifferentiated State of Cultured Satellite Cells

(A) Immunostaining of cultured satellite cells by the Matrigel control or the Pre3/4/5-on2 group for anti-PAX7 antibody (green), anti-MYOD antibody (red), and DAPI (blue). Scale bar represents 500 μm.

(B) The relative fluorescence intensity of PAX7 at day 5. The ratio of the Matrigel control was set as 1.0. n = 3 independent experiments. Error bars, SEM; **p < 0.01.

(C) The percentage of PAX7^{+}MYOD^{-} (blue), PAX7^{+}MYOD^{+} (pink), and PAX7^{-}MYOD^{+} (red) cells at day 5. n = 3 independent experiments. Error bars, SEM; *p < 0.05, **p < 0.01.

(D) The relative mRNA levels of *Myogenin* in satellite cells cultured on the Matrigel control and the Pre3/4/5-on2 condition at day 5. The ratio of the Matrigel control was set as 1.0. n = 3 independent experiments. Error bars, SEM; **p < 0.01.

(E) Number of PAX7^{+} satellite cells cultured on the Matrigel control and the Pre3/4/5-on2 group for 5 days. n = 3 independent experiments. Error bars, SEM; *p < 0.05.

(F) Ratio of Ki67^{+} proliferating cells in PAX7^{+} satellite cells cultured by the Matrigel control and the Pre3/4/5-on2 group for 5 days was calculated. n = 3 independent experiments. Error bars, SEM; *p < 0.05.

found that the ratios of PAX7^{+}MYOD^{-} (Figure 3C, blue bars) and PAX7^{+}MYOD^{+} (Figure 3C, pink bars) satellite cells were both higher in the Pre3/4/5-on2 group than in the Matrigel control. In contrast, the ratio of PAX7^{-}MYOD^{+} committed myogenic cells was significantly lower in Pre3/4/5-on2 (Figure 3C, red bars). In addition, the *Myogenin* mRNA level was lower in Pre3/4/5-on2 condition than in the Matrigel control (Figure 3D). These observations

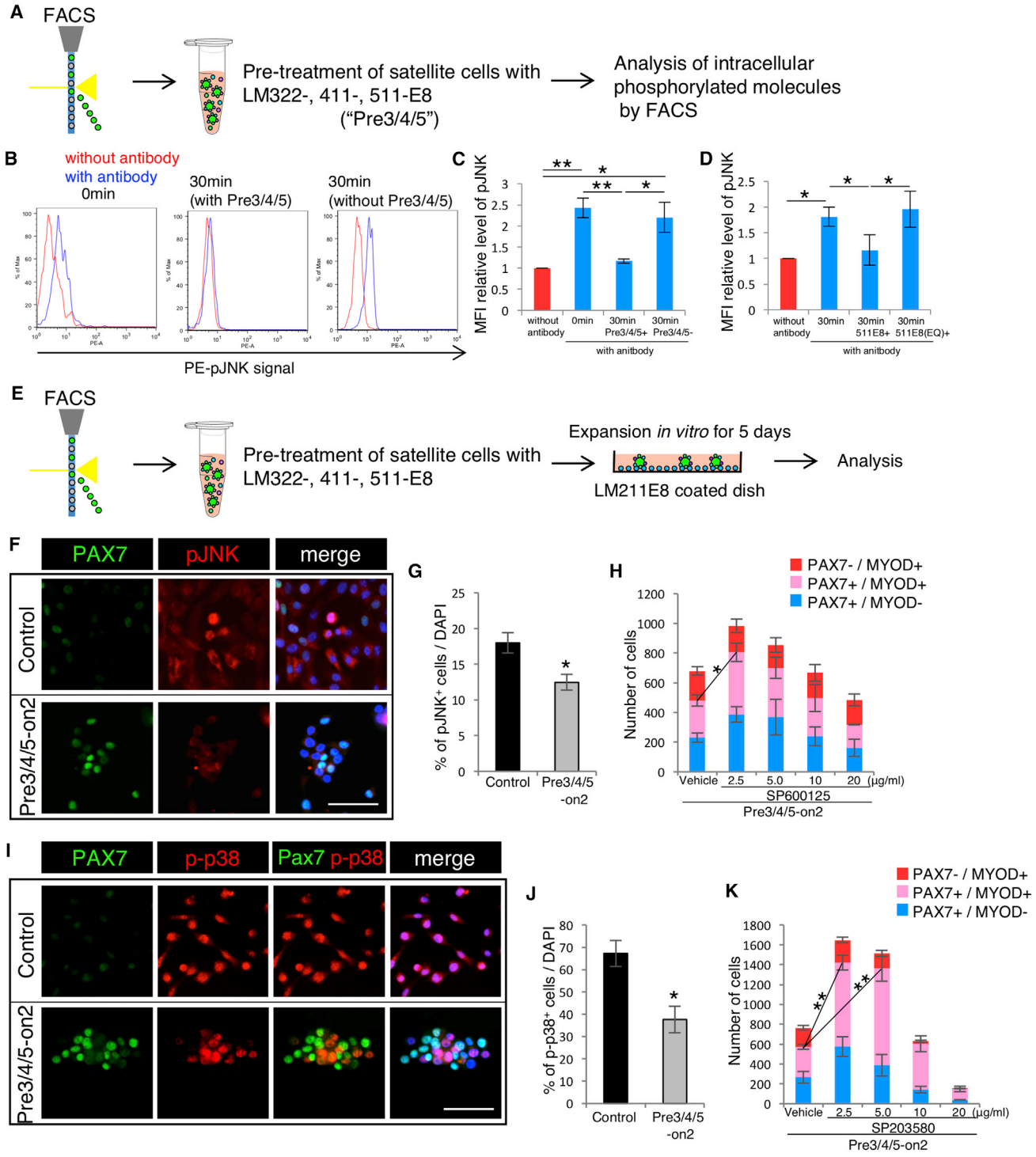

Figure 4. LM-E8 Fragments Mediate Activation of JNK and p38

(A) Levels of the phosphorylated molecules measured using FACS on isolated satellite cells with/without treatment with LM332-, 411-, and 511-E8 for 30 min.

(B) Histograms show levels of phosphorylated JNK. Blue line histogram; controls (without antibody) and red line histogram; samples (with antibody). Left: satellite cells after sorting. Middle: satellite cells treated with LM332-, 411-, and 511-E8 for 30 min after sorting. Right: satellite cells treated without LM332-, 411-, and 511-E8 for 30 min after sorting.

(legend continued on next page)

suggest that reconstitution of the LM environment maintains PAX7-expressing satellite cells in an undifferentiated state. We next investigated the effects of Pre3/4/5-on2 on the proliferative capacity of cultured satellite cells. We found that the number of $PAX7^+$ satellite cells was higher in the Pre3/4/5-on2 group than in the Matrigel control (Figure 3E). The percentage of proliferating cells marked by expression of KI67 within the population of $PAX7^+$ satellite cells was also higher in the Pre3/4/5-on2 group (Figure 3F), indicating that satellite cells maintain their proliferative capacity when grown in a Pre3/4/5-on2 environment. Under this culture condition, satellite cells exited the quiescent state and proliferated, while maintaining the expression of PAX7. Collectively, these results suggest that culture with LM-E8 prevents satellite cell differentiation and promotes proliferation, which may indirectly increase the satellite cell self-renewal pool.

LM-E8 Fragments Mediate the Activation of JNK in Satellite Cells

LM-E8 fragments include the INTEGRIN-binding sites of the intact LM protein (Miyazaki et al., 2012). To investigate downstream partners by LM-E8 in satellite cells and its role in maintaining the undifferentiated state of cultured satellite cells, we analyzed the downstream signaling of INTEGRINs. Immediately after isolating satellite cells by FACS, we measured phosphorylation levels of several intracellular signaling molecules (Figures 4A and S4). Interestingly, the level of phosphorylated JNK (pJNK) was elevated in sorted satellite cells, while the phosphorylation levels of other molecules (p38, ERK, FAK, STAT3, SRC, AKT, and p53) were unchanged (Figure S4), suggesting the involvement of JNK phosphorylation in the early stage of the activation of satellite cells. After treating sorted satellite cells with LM322-, 411-, and 511-E8, we observed dephosphorylation of JNK (Figures 4B and 4C). To determine whether this effect is mediated by INTEGRINs, we examined cells treated with fragments of LM511-E8 (EQ), in which the Glu residue (E) in the C-terminal tail region of the γ1 chain of LM511-E8 is replaced with Gln (Q) to prevent INTEGRIN binding (Miyazaki et al., 2012). We found that treatment with LM511-E8 (EQ) did not decrease the level of pJNK (Figure 4D). These results indicate that LME8-INTEGRIN signaling reduces the phosphorylation of JNK in isolated satellite cells.

JNK signaling promotes proliferation of satellite cells and differentiation of myoblasts during regenerative myogenesis (Alter et al., 2008; Shi et al., 2013). We next analyzed the level of pJNK in Pre3/4/5-on2-cultured satellite cells (Figure 4E). We found that the level of pJNK was reduced in the Pre3/4/5-on2 group compared with the Matrigel control (Figures 4F and 4G). To test for effective inhibition of JNK activity in Pre3/4/5-on2-cultured satellite cells, we examined various concentrations of JNK inhibitor SP600125. $PAX7^+$ satellite cells were increased at 2.5 μg/mL of SP600125, but were not significantly changed at concentrations >5.0 μg/mL (Figure 4H), suggesting that the moderate level of the inhibition in JNK signaling increased the number of $PAX7^+$ cells in the Pre3/4/5-on2. LM-E8-INTEGRIN signaling thus proliferates cultured satellite cells in an undifferentiated state through regulation of JNK activation.

Reconstitution of Extracellular LM Environment by LM-E8 Fragments Decreases the Activation of p38 in Satellite Cells

High levels of p38 activity promote differentiation (Bernet et al., 2014; Charville et al., 2015; Troy et al., 2012). We investigated whether phosphorylation of p38 in cultured

(C) Ratios of mean fluorescence intensities (MFIs), calculated based on FACS data. The ratio of the sample without antibody was set as 1.0. n = 3 independent experiments. Error bar, SEM; *p < 0.05, **p < 0.01.
(D) Ratio of phosphorylated JNK was measured by FACS sorting of isolated satellite cells incubated with/without LM511-E8 or LM511-E8 (EQ) for 30 min. MFIs were calculated based on FACS data. The ratio of the sample without antibody was set as 1.0. n = 3 independent experiments. Error bars, SEM; *p < 0.05.
(E) Sorted satellite cells cultured by the Matrigel control and the Pre3/4/5-on2 condition for 5 days.
(F) Immunostaining of satellite cells cultured on the Matrigel control and the Pre3/4/5-on2 condition for PAX7 (green), pJNK (red), and DAPI at 5 days. Scale bar represents 100 μm.
(G) Ratio of JNK phosphorylated cells to all cells. n = 3 independent experiments. Error bars, SEM; *p < 0.05.
(H) The number of $PAX7^+MYOD^-$ (blue), $PAX7^+MYOD^+$ (pink), and $PAX7^-MYOD^+$ (red) cells cultured by the Pre3/4/5-on2 group with 2.5, 5.0, 10, or 20 μg/mL SP600125 (JNK inhibitor) for 5 days were calculated. n = 3. Statistical analysis was performed on the number of $PAX7^+$ cells. Error bars, SEM; *p < 0.05.
(I) Immunostaining of satellite cells cultured by the Matrigel control and the Pre3/4/5-on2 condition for PAX7 (green), p-p38 (red), and DAPI at 5 days. Scale bar represents 100 μm.
(J) Ratio of p38 phosphorylated cells cultured on the Matrigel control and the Pre3/4/5-on2 group was calculated. n = 3 independent experiments. Error bars, SEM; *p < 0.05.
(K) The number of $PAX7^+MYOD^-$ (blue), $PAX7^+MYOD^+$ (pink), and $PAX7^-MYOD^+$ (red) cells cultured by the Pre3/4/5-on2 group with 2.5, 5.0, 10, or 20 μg/mL SP600125 (JNK inhibitor) for 5 days were calculated. n = 3 independent experiments. Statistical analysis was performed on the number of $PAX7^+$ cells. Error bars, SEM; **p < 0.01.

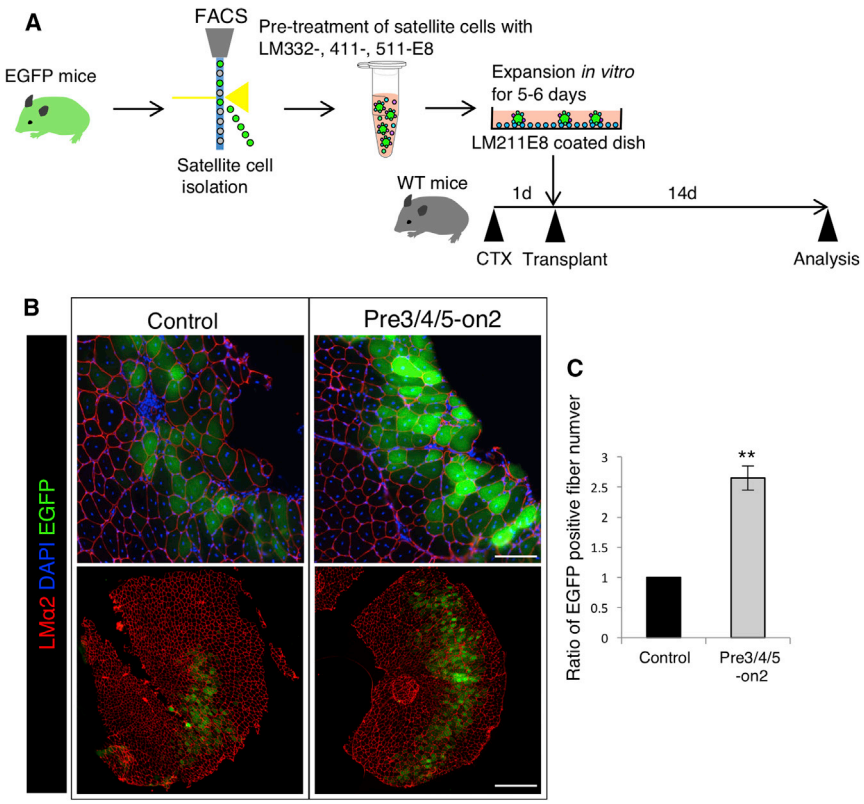

Figure 5. Satellite Cells Cultured by Pre3/4/5-on2 Enhance Regenerative Capacity

(A) EGFP-positive satellite cells were sorted and cultured by the Matrigel control and the Pre3/4/5-on2 group for 5 days. These cells were injected into C57BL/6 tibialis anterior (TA) muscles.

(B) Two weeks after the injection, cross-sections were stained with LMα2 (red) and DAPI (blue). Scale bars represent 100 μm (upper figures) and 500 μm (lower figures).

(C) Number of EGFP-positive fibers in TA muscle was calculated. The ratio of the Matrigel control was set as 1.0. n = 3 independent experiments. Error bars, SEM; **p < 0.01.

satellite cells is regulated by Pre3/4/5-on2. We found that levels of phosphorylated p38 were reduced in Pre3/4/5-on2 cultured cells (Figures 4I and 4J), indicating that LM-E8 directly or indirectly attenuates p38 activation. Interestingly, inversely proportional levels of PAX7 expression and p38 phosphorylation were observed in cultured satellite cells in the Pre3/4/5-on2 group, whereas nearly all cultured satellite cells were observed with phosphorylation of p38 on Matrigel (Figure 4I). To investigate the role of p38 signaling in the proliferation of satellite cells in an undifferentiated state in the Pre3/4/5-on2 culture, we analyzed the expression level of PAX7 in cultured satellite cells using an inhibitor of p38, SB203580 (Charville et al., 2015; Hayashiji et al., 2015), in various concentrations. $PAX7^+$cells were increased at 2.5 and 5.0 μg/mL of SP203580, but decreased at 20 μg/mL (Figure 4H). As with JNK inhibition, moderate levels of p38 inhibition increased the number of $PAX7^+$cells. These results suggest that Pre3/4/5-on2 culture maintains undifferentiated state in cultured satellite cells in an undifferentiated state, at least in part through regulation of p38 phosphorylation.

LM-E8 Fragments Enhance the Efficiency of Satellite Cell Transplantation

To analyze the regenerative efficiency of satellite cells cultured on Pre3/4/5-on2, cultured satellite cells isolated from C57BL/6-EGFP mice were injected with 2×10^5 cells per TA muscle of 8-week-old wild-type C57BL/6 mice (Figure 5A). Twenty-four hours before transplantation, recipient C57BL/6 muscles were injected with cardiotoxin to induce tissue damage and initiate the regenerative response. Two weeks after transplantation, we investigated the contribution of the transplanted cells to the regeneration of muscle tissue by detection of EGFP-positive fibers (Figure 5B). These fluorescence signals were not derived from autofluorescence in the tissue (Figure S5). Transplantation of satellite cells cultured in Pre3/4/5-on2 produced significantly more EGFP-positive fibers than those cultured on the Matrigel control (Figure 5C), suggesting that satellite cells cultured in Pre3/4/5-on2 exhibit enhanced ability to contribute to regeneration.

In Human Muscle Tissue, Satellite Cells Are Encapsulated in LMα3, α4, and α5

To identify the immunohistochemical localization of each LM α chain in human skeletal muscle, semitendinosus muscles were stained with antibodies against each LM α chain and against PAX7. LMα2 staining labeled muscle basement membrane, as expected. $PAX7^+$ satellite cells were located adjacent to the basement membrane (Figure 6A, arrowheads). $PAX7^+$ satellite cells were surrounded by LMα3, α4, and α5, forming a microenvironment similar

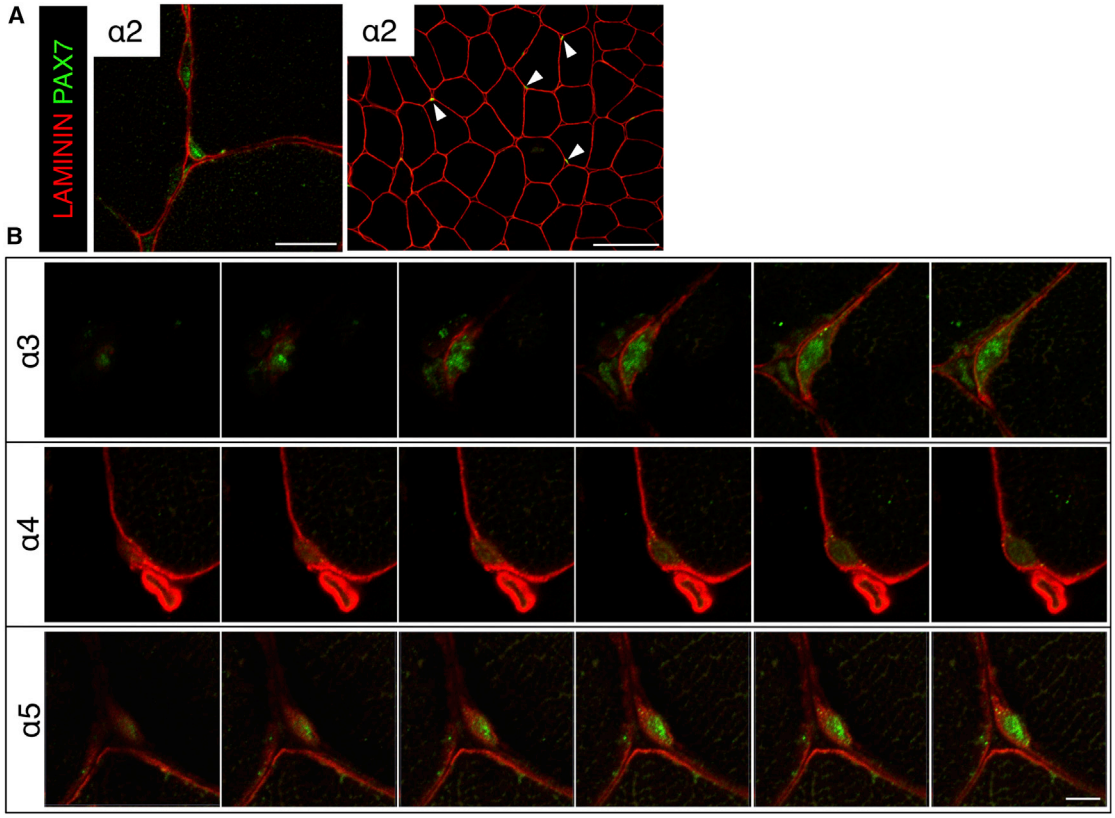

Figure 6. Expression of LM α Chains in Human Skeletal Muscle

(A) LM immunofluorescence using anti-α2 chain antibodies is shown in red. PAX7 was used as satellite cell maker (green) and DAPI was used a nuclear maker (blue). Left panel shows lower magnification images. Arrowheads indicate PAX7$^+$ cells located between a myofiber and basement membrane, labeled with LMα2 staining. Scale bars represent 50 μm (left figure) and 100 μm (right figure).

(B) High-magnification view of LMα3, α4, and α5 expression around satellite cells. Scale bar represents 5 μm.

to that observed in mouse (Figure 6B). As was the case in mouse, LMα1 was not detected in human muscle tissue (data not shown). Strong immunostaining of LMα4 was detected in the basement membrane of blood vessels as well. These results indicate that satellite cells are encapsulated in LMα3, α4, and α5 in human skeletal muscle tissue, closely resembling the satellite cell microenvironment in mouse.

LM-E8 Fragments Expand Undifferentiated Satellite Cells and Enhance Regenerative Capacity of Human Satellite Cell

To analyze the effect of Pre3/4/5-on2 on human satellite cells, we cultured human satellite cells with Pre3/4/5-on2, following the same approach as used in our tests of mouse satellite cells described above (Figure 7A). We directly isolated mononuclear cells from human semitendinosus muscles by FACS using CD56 and INTEGRIN α7 antibodies (Figure S6) (Castiglioni et al., 2014). To analyze the effect of Pre3/4/5-on2 on maintenance of the undifferentiated state of human satellite cells, we first examined the PAX7$^+$ cell population in cultured human satellite cells. The relative fluorescence intensity of PAX7 was highest in the Pre3/4/5-on2 group compared with the Matrigel control (Figure 7B). These results suggest that functional reconstitution of the extracellular LM environment by LM-E8 promotes maintenance of undifferentiated satellite cells in human as well as in mouse.

We next cultured human satellite cells with StemFit, a clinical-grade defined culture medium developed for use in clinical application, to assess the robustness of Pre3/4/5-on2 in conditions closer to those required in translational and clinical research settings. We found that mRNA levels of *PAX7* increased in the Pre3/4/5-on2 group compared with the Matrigel control (Figure 7C). We also found that a ratio of satellite cells was increased in the Pre3/4/5-on2 group (Figure 7D). These results suggest that LM-E8 fragments expand the population of human satellite cells in an undifferentiated state.

To evaluate the ability of expanded human satellite cells to contribute to muscle regeneration, we injected

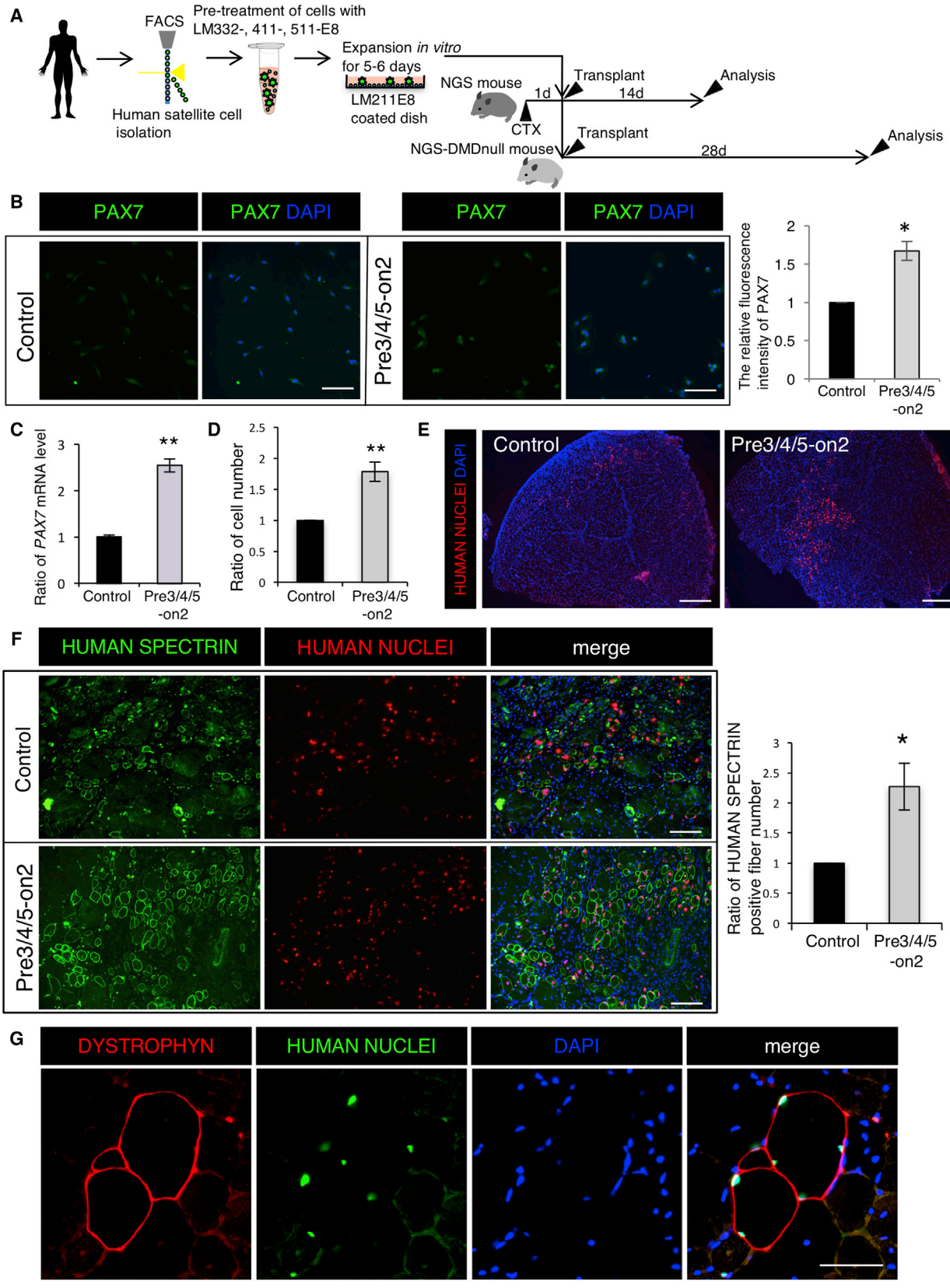

(legend on next page)

2–3 × 10^5 cells into the TA muscle of immunodeficient mice (NSG mice). Twenty-four hours before cell transplantation, we injected the recipient muscles with cardiotoxin to induce injury and trigger regeneration. Two weeks after injection, we prepared tissue sections and analyzed muscle regeneration by immunodetection of HUMAN NUCLEI- and HUMAN SPECTRIN-positive fibers. In three independent experiments, we observed more human nuclei in the TA muscle of NSG mice transplanted with cells cultured in Pre3/4/5-on2 than those grown on Matrigel (Figure 7E). We also observed 2–3 times as many HUMAN SPECTRIN-positive fibers in NSG mice transplanted satellite cells cultured in Pre3/4/5-on2 compared with the Matrigel control (Figure 7F). These data suggest that human satellite cells cultured in Pre3/4/5-on2 show enhanced engraftment and regenerative capacity.

Finally, we analyzed the regenerative ability of human satellite cells cultured in Pre3/4/5-on2 in DMD-null/NSG mice, which are severely immunodeficient and DYSTROPHIN deficient, and commonly used as a mouse model of DMD. Human satellite cells cultured in Pre3/4/5-on2 were injected into TA muscles of 10-week-old DMD-null/NSG mice at doses of 3 × 10^5 cells per muscle. Four weeks after injection, regenerated fibers, including cultured human satellite cells in Pre3/4/5-on2, were observed by immunodetection of DYSTROPHIN (Figure 7G). The antibody staining was specific, since the contralateral TA, used as a control, was not stained, indicating the specificity of this antibody staining (Figure S7). These results indicate that human satellite cells cultured in Pre3/4/5-on2 contribute to regeneration, even in DYSTROPHIN-deficient muscle.

In summary, the reconstitution of the extracellular LM environment by LM-E8 enables the *in vitro* expansion of undifferentiated human satellite cells, which retain their ability to contribute to tissue regeneration in mouse models of muscle defect and injury.

DISCUSSION

As a niche component, extracellular matrix in the surrounding microenvironment, or in direct cellular contact, has been shown to play important roles in maintaining quiescence, including satellite cells (Chen et al., 2013). In the present study, we established an artificial niche that maintains satellite cells *in vitro* using recombinant LM-E8 fragments. Our findings suggest that the recapitulation of the extracellular LM environment by LM-E8 supports proliferation of satellite cells in an undifferentiated state.

Satellite cell quiescence is required for the long-term maintenance of skeletal muscle homeostasis (Wang et al., 2014). Interactions between cells and ECM play important roles in tissues, including skeletal muscle. LMα2 is the most abundant LM isoform in the basement membrane of adult skeletal muscle (Yao et al., 1996). Our data show that satellite cells are encapsulated in LMα3, α4, and α5 (Figure 1). Thus, LMα3, α4, and α5, as well as LMα2, may play an important role as a niche for quiescent satellite cells. We found that the recapitulation of extracellular LM environment by LM-E8 maintains a pool of $PAX7^+$ satellite cells *in vitro* (Figure 2). In this culture condition, satellite cells exited the quiescent state and proliferated, while maintaining the expression of PAX7 (Figure 3). These observations suggest that other factors may be necessary for maintaining satellite cells in a quiescent state. In previous studies of cultured satellite cells, NOTCH signaling was shown to play a role in maintaining satellite cells, and is downregulated during differentiation (Bjornson et al., 2012; Conboy and Rando, 2002; Mourikis et al., 2012). Inhibition of the NOTCH signaling in satellite cells forces them to exit the quiescent state (Mourikis et al., 2012). In a myoblast cell line, constitutively active NOTCH delays the expression of the myogenic differentiation marker MYOD (Nofziger et al., 1999). One recent study suggested that synergy

Figure 7. LM-E8 Fragments Expand Undifferentiated Satellite Cells and Enhance Therapeutic Efficacy of Human Satellite Cell

(A) Sorted human satellite cells ($CD56^+$, $ITG\alpha7^+$ cells) cultured by the Matrigel control and the Pre3/4/5-on2 condition for 6 days.

(B) Immunostaining of human satellite cells cultured on the Matrigel control and the Pre3/4/5-on2 group for PAX7 (green) and (DAPI). Scale bar represents 100 μm. Bars show relative fluorescence intensity of PAX7 at day 6. The ratio of the Matrigel control was set at 1.0. n = 3 independent experiments. Error bars, SEM; *p < 0.05.

(C) The relative mRNA levels of *PAX7* in satellite cells cultured on the Matrigel control and the Pre3/4/5-on2 condition. The ratio of the Matrigel control was set as 1.0. n = 3 independent experiments. Pooled data from three individual human samples are shown. Error bars, SEM; **p < 0.01.

(D) Number of cultured satellite cells. The ratio of the Matrigel control was set as 1.0. n = 3 independent experiments. Error bars, SEM; **p < 0.01.

(E) Immunostaining of cross-section of TA muscle of NSG mice at 14 days after cardiotoxin injection for HUMAN NUCLEI antibody (red) and DAPI. Scale bar represents 500 μm.

(F) Immunostaining of cross-sections of TA muscle of NSG mice at 14 days after cardiotoxin injection for HUMAN SPECTRIN antibody (green), HUMAN NUCLEI antibody (red), and DAPI. Scale bar represents 100 μm. Bars show ratio of $HUMAN\ SPECTRIN^+$ fiber number. The ratio of the Matrigel control was set at 1.0. n = 3 independent experiments. Error bars, SEM; *p < 0.05.

(G) Immunostaining of cross-section of TA muscle of NSG-*mdx* mice at 28 days after cardiotoxin injection for DYSTROPHIN antibody (red), HUMAN NUCLEI antibody (green), and DAPI. Scale bar represents 100 μm.

between biomechanical and biochemical properties is required for the maintenance of PAX7 expression in satellite cells (Cosgrove et al., 2014). Activation, proliferation, and differentiation of satellite cells are regulated by changes in elastic stiffness *in vitro* (Boonen et al., 2009; Engler et al., 2006). To keep the quiescent state of satellite cells *in vitro*, it may even be necessary to mimic NOTCH signaling and elasticity.

To address the signals provided from LM-E8 fragments, we analyzed the phosphorylation of downstream signaling molecules (Figures 4 and S4). Our data reveal that satellite cells are maintained in an undifferentiated state through regulation of JNK and p38 signaling in LM-E8 culture (Figure 4). Members of the MAPK family regulate the activation, proliferation, and differentiation of satellite cells. JNK and p38 signaling is involved in the exit of satellite cells from quiescent state (Jones et al., 2005; Perdiguero et al., 2007; Troy et al., 2012). JNK signaling is involved in myoblast differentiation (Alter et al., 2008). The p38 pathway is required for the activation and differentiation of satellite cells and inducing the expression of MYOD (Jones et al., 2005). Low-level p38 activation is required for asymmetric division and self-renewal of satellite cells. Conversely, high levels of p38 activity promote differentiation (Bernet et al., 2014; Charville et al., 2015; Cosgrove et al., 2014). It has also been reported that the expression of *DUSP1* (dual-specificity phosphatase-1) is decreased upon activation of human satellite cells in culture (Charville et al., 2015). The DUSP1 protein has phosphatase activity, and specifically inactivates MAPK proteins, in particular JNK and p38. One previous study reported that ECM induces dephosphorylation of JNK and p38 (Givant-Horwitz et al., 2004). Crosstalk between intracellular signaling pathways is important for cell fate determination and the regulation of cellular responses to extracellular signals. One previous study reported that NOTCH specifically induces the expression of DUSP1, and directly inactivates p38 MAPK in the myogenic cell line (Kondoh et al., 2007). Moreover, LM-binding INTEGRINs specifically induce the expression of NOTCH ligands (Estrach et al., 2011). We thus suggest that the recapitulation of the extracellular LM environment by LM-E8 maintains satellite cells in an undifferentiated state via direct and/or indirect pathways.

In this study, we found that satellite cells behave differently when grown on Matrigel or LM-E8 culture, possibly due to differences in signals transmitted to satellite cells by LM-E8 and Matrigel, which contain many proteins, including full-length LMs. Our results also showed that treating satellite cells with LM332-, 411-, or 511-E8 on an LM211-E8-coated dish is important for maintaining them in an undifferentiated state. Previous studies have reported that satellite cells express high levels of α7β1 INTEGRIN, which binds to LMα2 (Burkin and Kaufman, 1999). Stem cells may be anchored to their niche via adhesion molecules to maintain the quiescent state and continuously self-renew (Chen et al., 2013). It was recently reported that LM521 supports formation of myotubes *in vitro* (Penton et al., 2016). Full-length LM521 acts synergistically on the RGD-dependent INTEGRIN-binding site and the α1β1/α2β1 INTEGRIN-binding site in the N-terminal region of the α5 chain, in addition to the INTEGRIN-binding site of the E8 region. These findings suggest that satellite cell responses to full-length LM and the LM-E8 fragment, which bind only to INTEGRIN, may differ. Binding between N-terminal domains of LM is important for the construction of the basement membrane, while the E8 region contains the INTEGRIN-binding sites, which may be involved in the maintenance of stem cells. Treatment with LM332-, 411-, or 511-E8 in the liquid phase, immediately after the isolation of cells from muscle tissue, may thus also provide a functional equivalent to the LM pericellular matrix for satellite cells in culture. The pericellular matrix plays important roles in regulating biomechanical, biophysical, and biochemical interactions between cells and the ECM. A previous study suggested that the pericellular matrix plays a key role in controlling cell homeostasis and maintaining the undifferentiated status of pluripotent cells (Guilak et al., 2006; Wilusz et al., 2014). Chondrogenic progenitor cells produce high levels of LMα1 and α5 in their pericellular matrix (Schminke et al., 2016). In skeletal muscle, COLLAGEN VI is expressed around satellite cells and also functions as a pericellular matrix (Urciuolo et al., 2013). Our results suggest that it is possible to reconstruct the pericellular LM environment by treatment with LME8 fragments, minimal fragments possessing INTEGRIN-binding activity in cell culture.

Importantly, we have also shown that satellite cells are encapsulated in LMα3, α4, and α5 in the human skeletal muscle tissue, and that LM211-, 332-, 411-, and 511-E8 fragments support the expansion of human satellite cells in an undifferentiated state. These results suggest that human satellite cells can be regulated by the recapitulation of the extracellular LM environment using recombinant LM-E8 fragments *in vitro*. This study thus provides an efficient method for preparing human satellite cells using recombinant proteins, with potential applications in the development of novel cell therapeutics.

EXPERIMENTAL PROCEDURES

Cell Culture

Isolated mouse satellite cells were plated on plastic dishes or glass chamber slides coated with Matrigel (BD Matrigel Matrix Growth Factor Reduced, BD Biosciences), gelatin (StemSure 0.1 w/v% Gelatin

Solution, Wako) or LM-E8 fragment. To promote proliferation, satellite cells were cultured in DMEM with GlutaMAX (Life Technologies) containing 20% fetal bovine serum (FBS) (Sigma-Aldrich), 1% chick embryo extract (United States Biological), 100 units/mL penicillin, 100 μg/mL streptomycin (Life Technologies), and 5 ng/mL basic fibroblast growth factor (ReproCell) in 5% CO_2 at 37°C. In the differentiation assay, satellite cells were cultured in differentiation medium consisting of DMEM with GlutaMAX supplemented with 5% horse serum (Life Technologies), 100 units/mL penicillin, and 100 μg/mL streptomycin. Human satellite cells were cultured in DMEM with GlutaMAX (Life Technologies) containing 20% FBS (Sigma-Aldrich), 100 units/mL penicillin, 100 μg/mL streptomycin (Life Technologies), with 5% horse serum (Life Technologies) and 25 ng/mL basic fibroblast growth factor (ReproCell) under 5% CO_2 at 37°C for 5 days. For transplantation, human satellite cells were cultured in Stemfit AN03K (Ajinimoto) under 5% CO_2 at 37°C for 6 days.

Cell Transplantation

To induce muscle injury, cardiotoxin (Sigma-Aldrich) was injected into the TA muscles of C57BL/6 mice, NSG mice, or DMD-null/NSG mice 24 hr before transplantation. Independent C57BL/6-GFP transgenic mouse- and human-derived satellite cells cultured on Matrigel or LM-E8 (Pre3/4/5-on2) for 5 days were injected directly into the TA muscle.

SUPPLEMENTAL INFORMATION

Supplemental Information includes Supplemental Experimental Procedures and seven figures and can be found with this article online at https://doi.org/10.1016/j.stemcr.2017.12.013.

AUTHOR CONTRIBUTIONS

K.I. designed the experiments, analyzed the data, and wrote the manuscript. H.S. performed the cell transplantation assay, analyzed the data, oversaw the results, and wrote the manuscript. N.S. designed the experiments, analyzed the data, oversaw the results, and wrote the manuscript. Y.M. performed the FACS assay, analyzed the data, and oversaw the results. K.S. designed and prepared the LM-E8 fragments, analyzed the data, and oversaw the results. I.S. provided support for the human samples and oversaw the results. C.A. coordinated the study, oversaw the results, wrote the manuscript, and finally approved the manuscript.

ACKNOWLEDGMENTS

We thank So-ichiro Fukada (Osaka University, Osaka, Japan) for providing the SM/C-2,6 antibody. We thank Naoki Ito and Eriko Grace Suto for technical advice and Naomi Kikura and Kirika Murakami for technical assistance. We thank Douglas Sipp (RIKEN CDB, Kobe, Japan) for his assistance in copyediting the manuscript. K.I. was funded by a Research Fellowship (JP 16J08994) from JSPS. This work was supported by Building of Consortia for the Development of Human Resources in Science and Technology, MEXT, and the Project for Practical Applications of Regenerative Medicine from AMED. Correspondence regarding LM-E8 fragments should be addressed to K.S. (sekiguch@protein.osaka-u.ac.jp).

Received: June 27, 2017
Revised: December 15, 2017
Accepted: December 15, 2017
Published: January 11, 2018

REFERENCES

Alter, J., Rozentzweig, D., and Bengal, E. (2008). Inhibition of myoblast differentiation by tumor necrosis factor alpha is mediated by c-Jun N-terminal kinase 1 and leukemia inhibitory factor. J. Biol. Chem. *283*, 23224–23234.

Bentzinger, C.F., Wang, Y.X., von Maltzahn, J., Soleimani, V.D., Yin, H., and Rudnicki, M.A. (2013). Fibronectin regulates Wnt7a signaling and satellite cell expansion. Cell Stem Cell *12*, 75–87.

Bernet, J.D., Doles, J.D., Hall, J.K., Kelly Tanaka, K., Carter, T.A., and Olwin, B.B. (2014). p38 MAPK signaling underlies a cell-autonomous loss of stem cell self-renewal in skeletal muscle of aged mice. Nat. Med. *20*, 265–271.

Bjornson, C.R., Cheung, T.H., Liu, L., Tripathi, P.V., Steeper, K.M., and Rando, T.A. (2012). Notch signaling is necessary to maintain quiescence in adult muscle stem cells. Stem Cells *30*, 232–242.

Boonen, K.J., Rosaria-Chak, K.Y., Baaijens, F.P., van der Schaft, D.W., and Post, M.J. (2009). Essential environmental cues from the satellite cell niche: optimizing proliferation and differentiation. Am. J. Physiol. Cell Physiol. *296*, C1338–C1345.

Burkin, D.J., and Kaufman, S.J. (1999). The alpha7beta1 integrin in muscle development and disease. Cell Tissue Res. *296*, 183–190.

Castiglioni, A., Hettmer, S., Lynes, M.D., Rao, T.N., Tchessalova, D., Sinha, I., Lee, B.T., Tseng, Y.H., and Wagers, A.J. (2014). Isolation of progenitors that exhibit myogenic/osteogenic bipotency in vitro by fluorescence-activated cell sorting from human fetal muscle. Stem Cell Reports *2*, 92–106.

Chargé, S.B., and Rudnicki, M.A. (2004). Cellular and molecular regulation of muscle regeneration. Physiol. Rev. *84*, 209–238.

Charville, G.W., Cheung, T.H., Yoo, B., Santos, P.J., Lee, G.K., Shrager, J.B., and Rando, T.A. (2015). Ex vivo expansion and in vivo self-renewal of human muscle stem cells. Stem Cell Reports *5*, 621–632.

Chen, S., Lewallen, M., and Xie, T. (2013). Adhesion in the stem cell niche: biological roles and regulation. Development *140*, 255–265.

Conboy, I.M., and Rando, T.A. (2002). The regulation of Notch signaling controls satellite cell activation and cell fate determination in postnatal myogenesis. Dev. Cell *3*, 397–409.

Cosgrove, B.D., Gilbert, P.M., Porpiglia, E., Mourkioti, F., Lee, S.P., Corbel, S.Y., Llewellyn, M.E., Delp, S.L., and Blau, H.M. (2014). Rejuvenation of the muscle stem cell population restores strength to injured aged muscles. Nat. Med. *20*, 255–264.

Danoviz, M.E., and Yablonka-Reuveni, Z. (2012). Skeletal muscle satellite cells: background and methods for isolation and analysis in a primary culture system. Methods Mol. Biol. *798*, 21–52.

Disatnik, M.H., and Rando, T.A. (1999). Integrin-mediated muscle cell spreading. The role of protein kinase c in outside-in and inside-out signaling and evidence of integrin cross-talk. J. Biol. Chem. *274*, 32486–32492.

Domogatskaya, A., Rodin, S., and Tryggvason, K. (2012). Functional diversity of laminins. Annu. Rev. Cell Dev. Biol. *28*, 523–553.

Dumont, N.A., Wang, Y.X., and Rudnicki, M.A. (2015). Intrinsic and extrinsic mechanisms regulating satellite cell function. Development *142*, 1572–1581.

Engler, A.J., Sen, S., Sweeney, H.L., and Discher, D.E. (2006). Matrix elasticity directs stem cell lineage specification. Cell *126*, 677–689.

Estrach, S., Cailleteau, L., Franco, C.A., Gerhardt, H., Stefani, C., Lemichez, E., Gagnoux-Palacios, L., Meneguzzi, G., and Mettouchi, A. (2011). Laminin-binding integrins induce Dll4 expression and Notch signaling in endothelial cells. Circ. Res. *109*, 172–182.

Fukada, S., Higuchi, S., Segawa, M., Koda, K., Yamamoto, Y., Tsujikawa, K., Kohama, Y., Uezumi, A., Imamura, M., Miyagoe-Suzuki, Y., et al. (2004). Purification and cell-surface marker characterization of quiescent satellite cells from murine skeletal muscle by a novel monoclonal antibody. Exp. Cell Res. *296*, 245–255.

Gilbert, P.M., Havenstrite, K.L., Magnusson, K.E., Sacco, A., Leonardi, N.A., Kraft, P., Nguyen, N.K., Thrun, S., Lutolf, M.P., and Blau, H.M. (2010). Substrate elasticity regulates skeletal muscle stem cell self-renewal in culture. Science *329*, 1078–1081.

Givant-Horwitz, V., Davidson, B., and Reich, R. (2004). Laminin-induced signaling in tumor cells: the role of the M(r) 67,000 laminin receptor. Cancer Res. *64*, 3572–3579.

Grefte, S., Vullinghs, S., Kuijpers-Jagtman, A.M., Torensma, R., and Von den Hoff, J.W. (2012). Matrigel, but not collagen I, maintains the differentiation capacity of muscle derived cells in vitro. Biomed. Mater. *7*, 055004.

Guilak, F., Alexopoulos, L.G., Upton, M.L., Youn, I., Choi, J.B., Cao, L., Setton, L.A., and Haider, M.A. (2006). The pericellular matrix as a transducer of biomechanical and biochemical signals in articular cartilage. Ann. N. Y. Acad. Sci. *1068*, 498–512.

Guo, L.T., Zhang, X.U., Kuang, W., Xu, H., Liu, L.A., Vilquin, J.T., Miyagoe-Suzuki, Y., Takeda, S., Ruegg, M.A., Wewer, U.M., et al. (2003). Laminin alpha2 deficiency and muscular dystrophy; genotype-phenotype correlation in mutant mice. Neuromuscul. Disord. *13*, 207–215.

Hayashiji, N., Yuasa, S., Miyagoe-Suzuki, Y., Hara, M., Ito, N., Hashimoto, H., Kusumoto, D., Seki, T., Tohyama, S., Kodaira, M., et al. (2015). G-CSF supports long-term muscle regeneration in mouse models of muscular dystrophy. Nat. Commun. *6*, 6745.

Helbling-Leclerc, A., Zhang, X., Topaloglu, H., Cruaud, C., Tesson, F., Weissenbach, J., Tomé, F.M., Schwartz, K., Fardeau, M., Tryggvason, K., et al. (1995). Mutations in the laminin alpha 2-chain gene (LAMA2) cause merosin-deficient congenital muscular dystrophy. Nat. Genet. *11*, 216–218.

Heng, C., Lefebvre, O., Klein, A., Edwards, M.M., Simon-Assmann, P., Orend, G., and Bagnard, D. (2011). Functional role of laminin alpha1 chain during cerebellum development. Cell Adh. Migr. *5*, 480–489.

Holmberg, J., and Durbeej, M. (2013). Laminin-211 in skeletal muscle function. Cell Adh. Migr. *7*, 111–121.

Ikemoto, M., Fukada, S., Uezumi, A., Masuda, S., Miyoshi, H., Yamamoto, H., Wada, M.R., Masubuchi, N., Miyagoe-Suzuki, Y., and Takeda, S. (2007). Autologous transplantation of SM/C-2.6(+) satellite cells transduced with micro-dystrophin CS1 cDNA by lentiviral vector into mdx mice. Mol. Ther. *15*, 2178–2185.

Johansson, S., Svineng, G., Wennerberg, K., Armulik, A., and Lohikangas, L. (1997). Fibronectin-integrin interactions. Front. Biosci. *2*, d126–d146.

Jones, N.C., Tyner, K.J., Nibarger, L., Stanley, H.M., Cornelison, D.D., Fedorov, Y.V., and Olwin, B.B. (2005). The p38alpha/beta MAPK functions as a molecular switch to activate the quiescent satellite cell. J. Cell Biol. *169*, 105–116.

Kondoh, K., Sunadome, K., and Nishida, E. (2007). Notch signaling suppresses p38 MAPK activity via induction of MKP-1 in myogenesis. J. Biol. Chem. *282*, 3058–3065.

Kuang, S., and Rudnicki, M.A. (2008). The emerging biology of satellite cells and their therapeutic potential. Trends Mol. Med. *14*, 82–91.

Kuang, S., Gillespie, M.A., and Rudnicki, M.A. (2008). Niche regulation of muscle satellite cell self-renewal and differentiation. Cell Stem Cell *2*, 22–31.

Lepper, C., Partridge, T.A., and Fan, C.M. (2011). An absolute requirement for Pax7-positive satellite cells in acute injury-induced skeletal muscle regeneration. Development *138*, 3639–3646.

Mauro, A. (1961). Satellite cell of skeletal muscle fibers. J. Biophys. Biochem. Cytol. *9*, 493–495.

Miner, J.H., and Yurchenco, P.D. (2004). Laminin functions in tissue morphogenesis. Annu. Rev. Cell Dev. Biol. *20*, 255–284.

Miyazaki, T., Futaki, S., Suemori, H., Taniguchi, Y., Yamada, M., Kawasaki, M., Hayashi, M., Kumagai, H., Nakatsuji, N., Sekiguchi, K., et al. (2012). Laminin E8 fragments support efficient adhesion and expansion of dissociated human pluripotent stem cells. Nat. Commun. *3*, 1236.

Montarras, D., Morgan, J., Collins, C., Relaix, F., Zaffran, S., Cumano, A., Partridge, T., and Buckingham, M. (2005). Direct isolation of satellite cells for skeletal muscle regeneration. Science *309*, 2064–2067.

Motohashi, N., Asakura, Y., and Asakura, A. (2014). Isolation, culture, and transplantation of muscle satellite cells. J. Vis. Exp. https://doi.org/10.3791/50846.

Mourikis, P., Sambasivan, R., Castel, D., Rocheteau, P., Bizzarro, V., and Tajbakhsh, S. (2012). A critical requirement for notch signaling in maintenance of the quiescent skeletal muscle stem cell state. Stem Cells *30*, 243–252.

Nofziger, D., Miyamoto, A., Lyons, K.M., and Weinmaster, G. (1999). Notch signaling imposes two distinct blocks in the differentiation of C2C12 myoblasts. Development *126*, 1689–1702.

Olguin, H.C., and Olwin, B.B. (2004). Pax-7 up-regulation inhibits myogenesis and cell cycle progression in satellite cells: a potential mechanism for self-renewal. Dev. Biol. *275*, 375–388.

Parker, M.H., Loretz, C., Tyler, A.E., Duddy, W.J., Hall, J.K., Olwin, B.B., Bernstein, I.D., Storb, R., and Tapscott, S.J. (2012). Activation of Notch signaling during ex vivo expansion maintains donor muscle cell engraftment. Stem Cells *30*, 2212–2220.

Patton, B.L., Connoll, A.M., Martin, P.T., Cunningham, J.M., Mehta, S., Pestronk, A., Miner, J.H., and Sanes, J.R. (1999).

Distribution of ten laminin chains in dystrophic and regenerating muscles. Neuromuscul. Disord. *9*, 423–433.

Penton, C.M., Badarinarayana, V., Prisco, J., Powers, E., Pincus, M., Allen, R.E., and August, P.R. (2016). Laminin 521 maintains differentiation potential of mouse and human satellite cell-derived myoblasts during long-term culture expansion. Skelet. Muscle *6*, 44.

Perdiguero, E., Ruiz-Bonilla, V., Serrano, A.L., and Muñoz-Cánoves, P. (2007). Genetic deficiency of p38alpha reveals its critical role in myoblast cell cycle exit: the p38alpha-JNK connection. Cell Cycle *6*, 1298–1303.

Relaix, F., and Zammit, P.S. (2012). Satellite cells are essential for skeletal muscle regeneration: the cell on the edge returns centre stage. Development *139*, 2845–2856.

Sambasivan, R., and Tajbakhsh, S. (2007). Skeletal muscle stem cell birth and properties. Semin. Cell Dev. Biol. *18*, 870–882.

Sambasivan, R., Yao, R., Kissenpfennig, A., Van Wittenberghe, L., Paldi, A., Gayraud-Morel, B., Guenou, H., Malissen, B., Tajbakhsh, S., and Galy, A. (2011). Pax7-expressing satellite cells are indispensable for adult skeletal muscle regeneration. Development *138*, 3647–3656.

Schminke, B., Frese, J., Bode, C., Goldring, M.B., and Miosge, N. (2016). Laminins and nidogens in the pericellular matrix of chondrocytes: their role in osteoarthritis and chondrogenic differentiation. Am. J. Pathol. *186*, 410–418.

Shi, H., Verma, M., Zhang, L., Dong, C., Flavell, R.A., and Bennett, A.M. (2013). Improved regenerative myogenesis and muscular dystrophy in mice lacking Mkp5. J. Clin. Invest. *123*, 2064–2077.

Tedesco, F.S., Dellavalle, A., Diaz-Manera, J., Messina, G., and Cossu, G. (2010). Repairing skeletal muscle: regenerative potential of skeletal muscle stem cells. J. Clin. Invest. *120*, 11–19.

Thomas, K., Engler, A.J., and Meyer, G.A. (2015). Extracellular matrix regulation in the muscle satellite cell niche. Connect. Tissue Res. *56*, 1–8.

Troy, A., Cadwallader, A.B., Fedorov, Y., Tyner, K., Tanaka, K.K., and Olwin, B.B. (2012). Coordination of satellite cell activation and self-renewal by Par-complex-dependent asymmetric activation of p38alpha/beta MAPK. Cell Stem Cell *11*, 541–553.

Urciuolo, A., Quarta, M., Morbidoni, V., Gattazzo, F., Molon, S., Grumati, P., Montemurro, F., Tedesco, F.S., Blaauw, B., Cossu, G., et al. (2013). Collagen VI regulates satellite cell self-renewal and muscle regeneration. Nat. Commun. *4*, 1964.

von Maltzahn, J., Jones, A.E., Parks, R.J., and Rudnicki, M.A. (2013). Pax7 is critical for the normal function of satellite cells in adult skeletal muscle. Proc. Natl. Acad. Sci. USA *110*, 16474–16479.

Wang, Y.X., Dumont, N.A., and Rudnicki, M.A. (2014). Muscle stem cells at a glance. J. Cell Sci. *127*, 4543–4548.

Wilusz, R.E., Sanchez-Adams, J., and Guilak, F. (2014). The structure and function of the pericellular matrix of articular cartilage. Matrix Biol. *39*, 25–32.

Yao, C.C., Ziober, B.L., Squillace, R.M., and Kramer, R.H. (1996). Alpha7 integrin mediates cell adhesion and migration on specific laminin isoforms. J. Biol. Chem. *271*, 25598–25603.

Zammit, P.S., Heslop, L., Hudon, V., Rosenblatt, J.D., Tajbakhsh, S., Buckingham, M.E., Beauchamp, J.R., and Partridge, T.A. (2002). Kinetics of myoblast proliferation show that resident satellite cells are competent to fully regenerate skeletal muscle fibers. Exp. Cell Res. *281*, 39–49.

Zammit, P.S., Golding, J.P., Nagata, Y., Hudon, V., Partridge, T.A., and Beauchamp, J.R. (2004). Muscle satellite cells adopt divergent fates: a mechanism for self-renewal? J. Cell Biol. *166*, 347–357.

Zou, K., De Lisio, M., Huntsman, H.D., Pincu, Y., Mahmassani, Z., Miller, M., Olatunbosun, D., Jensen, T., and Boppart, M.D. (2014). Laminin-111 improves skeletal muscle stem cell quantity and function following eccentric exercise. Stem Cells Transl. Med. *3*, 1013–1022.

Stem Cell Reports, Volume *10*

Supplemental Information

Recapitulation of Extracellular LAMININ Environment Maintains Stemness of Satellite Cells *In Vitro*

Kana Ishii, Hidetoshi Sakurai, Nobuharu Suzuki, Yo Mabuchi, Ichiro Sekiya, Kiyotoshi Sekiguchi, and Chihiro Akazawa

Figure S1

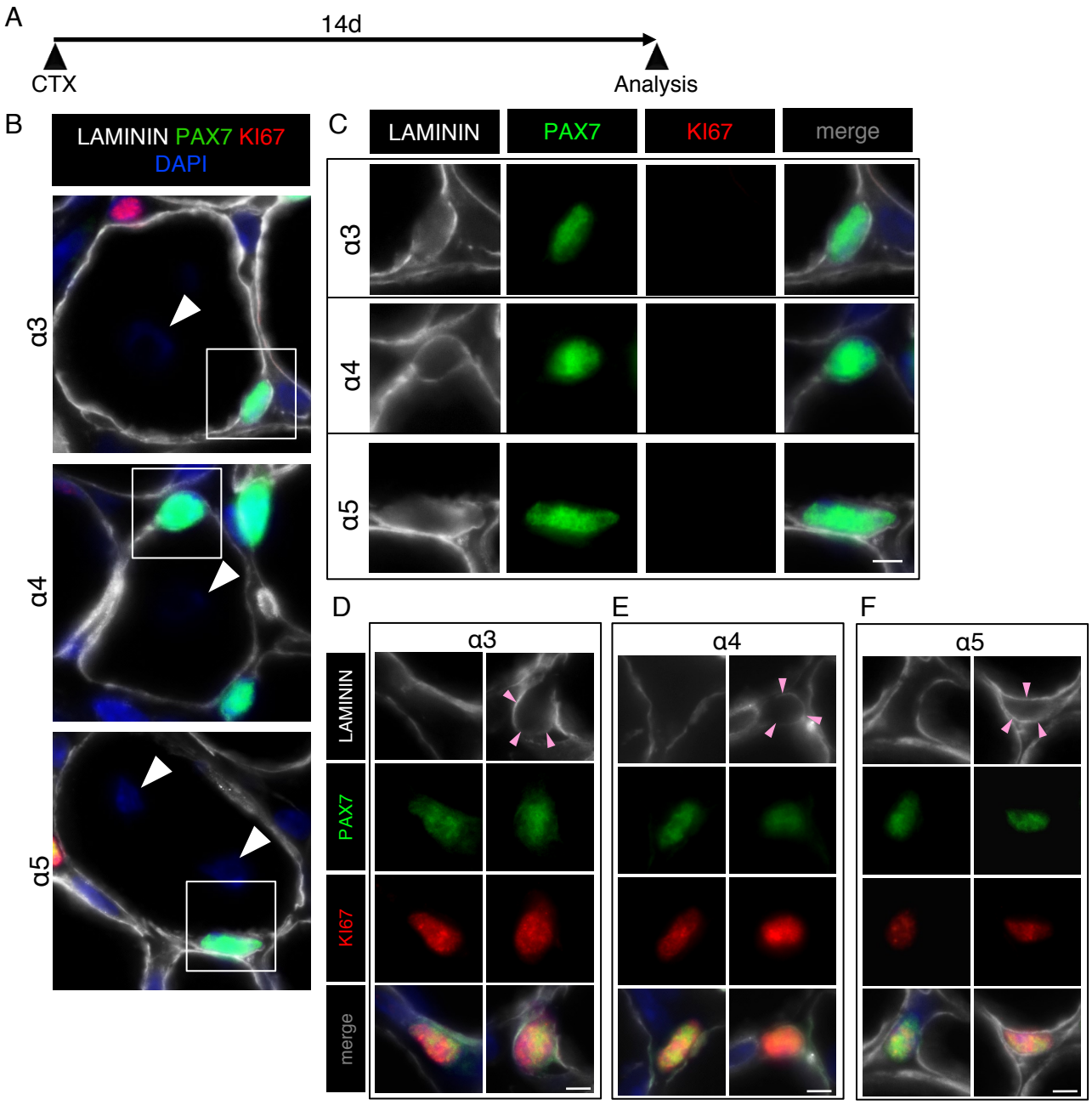

Figure S1. Expression patterns of LMa3, a4, and a5 around self-renewed and activated satellite cells. (A) Sections were obtained from TA muscle 14 days after CTX injection. (B-C) Expression patterns of LMa3, a4, and a5 around PAX7+KI67– self-renewed satellite cells after CTX injection. Muscle tissue stained with anti-PAX7 antibody (green), anti-KI67 antibody (red), and anti-LMa3-5 antibody (white). Arrowheads indicate the centrally located nuclei in regenerated fibers. Scale bar represents 10 μm. (D–F) Expression patterns of LMa3, a4, and a5 around $PAX7^{+}KI67^{+}$ activated satellite cells after CTX injection. Muscle tissue stained with anti-PAX7 antibody (green), anti-KI67 antibody (red) and anti-LMa3–5 antibody (white). Arrowheads indicate expression of LMα3, α4 and α5 around activated satellite cells. Scale bar represents 10 μm.

Figure S2

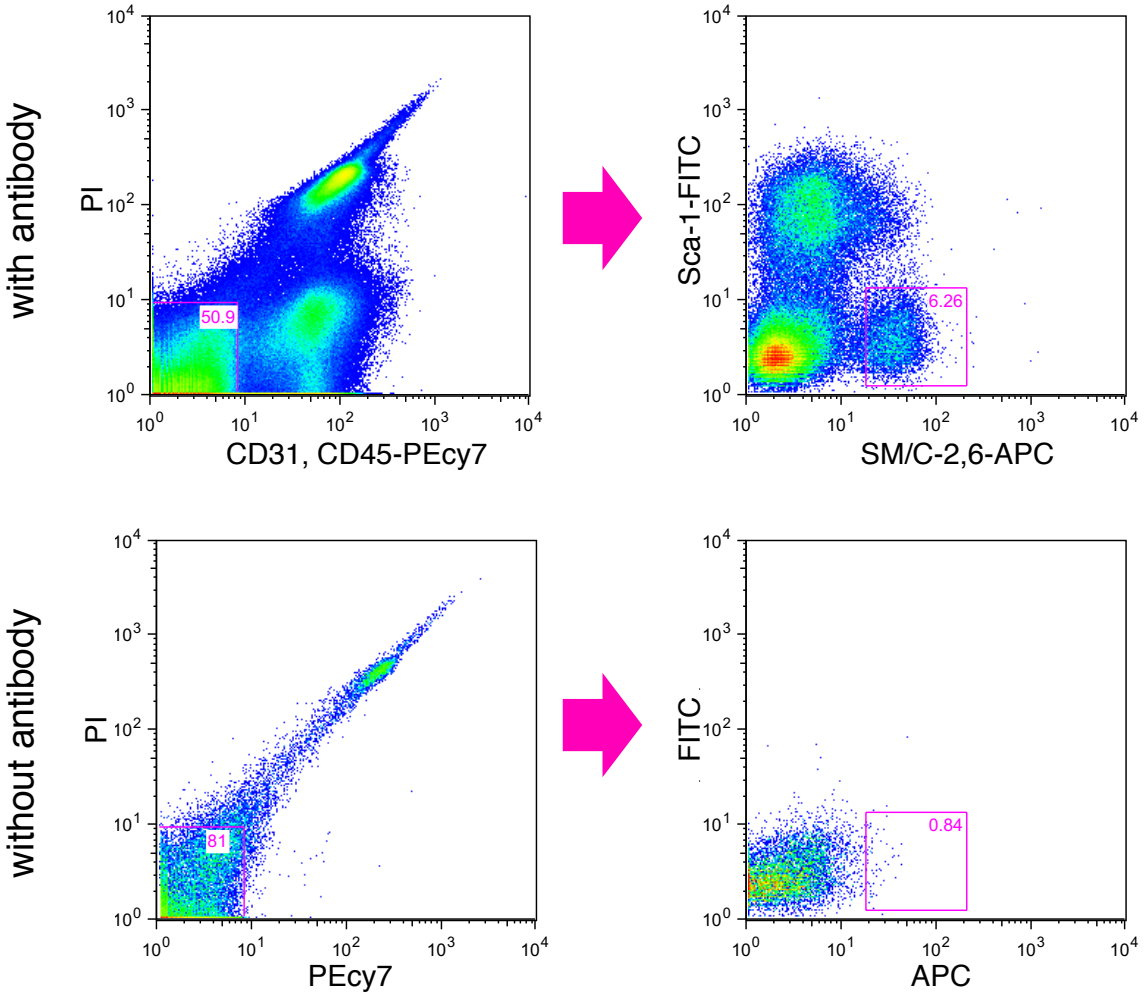

Figure S2. FACS profiles of satellite cells from WT mice. CD31−CD45−Sca-1−SM/C-2.6+ cells were analyzed as muscle satellite cells using MoFlo.

Figure S3

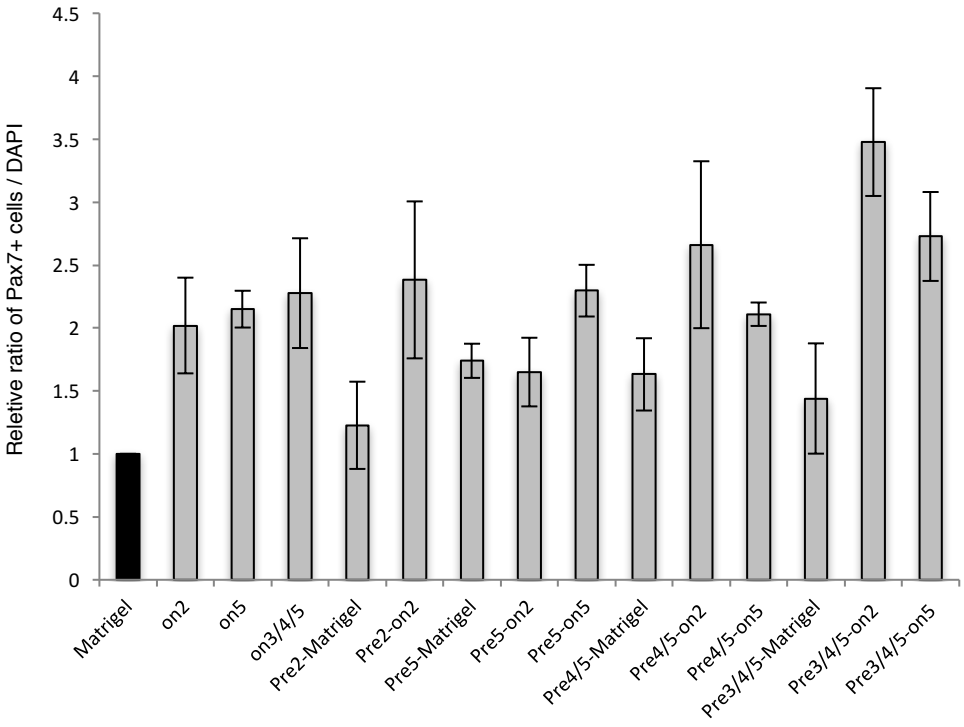

Figure S3. The ratio of PAX7 positive cells in several different culture conditions using the LME8 fragments. Matrigel; cultured on Matrigel coating dish (control), on2; cultured on LM211-E8 coated dish, on5; cultured on LM511-E8 coated dish, on3/4/5; cultured on LM332-, 411- and 511-E8 coated dish, Pre2-Matrigel; cultured on Matrigel coated dish after pre-treated with LM211-E8, Pre2-on2; cultured on LM211-E8 coated dish after pre-treated with LM211-E8, Pre5-Matrigel; cultured on Matrigel coated dish after pre-treated with LM511-E8, Pre5-on2; cultured on LM211-E8 coated dish after pre-treated with LM511-E8, Pre5-on5; cultured on LM511-E8 coated dish after pre-treated with LM511-E8, Pre4/5-Matrigel; cultured on Matrigel coated dish after pre-treated with LM411- and 511-E8, Prelm4/5-lm2; cultured on LM211-E8 coated dish after pre-treated with LM411- and 511- E8, Prelm4/5-lm5; cultured on LM511-E8 coated dish after pre-treated with LM411- and 511-E8, Prelm3/4/5-mt; cultured on Matrigel coated dish after pre-treated with LM332-, 411- and 511-E8, Prelm3/4/5-lm2; cultured on LM211-E8 coated dish after pre-treated with LM332-, 411- and 511- E8, Prelm3/4/5-lm5; cultured on LM511-E8 coated dish after pre-treated with LM332-, 411- and 511-E8. The ratio of the Matrigel was set as 1.0. Error bars, s.e.m.

Figure S4

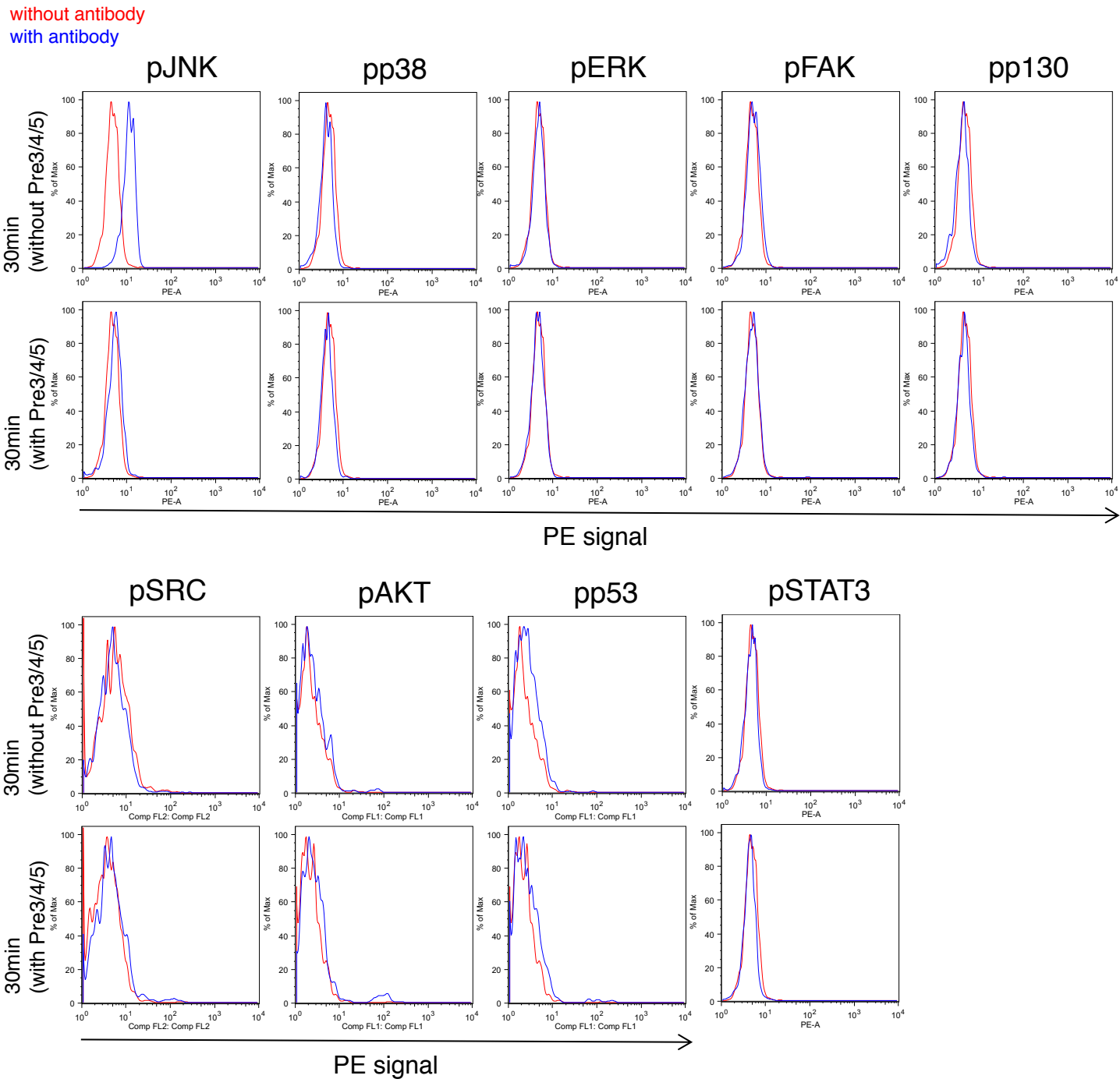

Figure S4. The phosphorylation levels of JNK, ERK, FAK, p38, p130, STAT3, SRC, AKT and p53 in satellite cells. Expression of phosphorylated molecules JNK, ERK, FAK, p38, p130, STAT3, SRC, AKT and p53 were measured by FACS on isolated satellite cells incubated with/without LM332-E8, 411-E8, and 511-E8 for 30 minutes. Histograms represent levels of protein expression. Blue line histogram; controls (without antibodies) and red line histogram; samples (incubated with/without LM-E8).

Figure S5

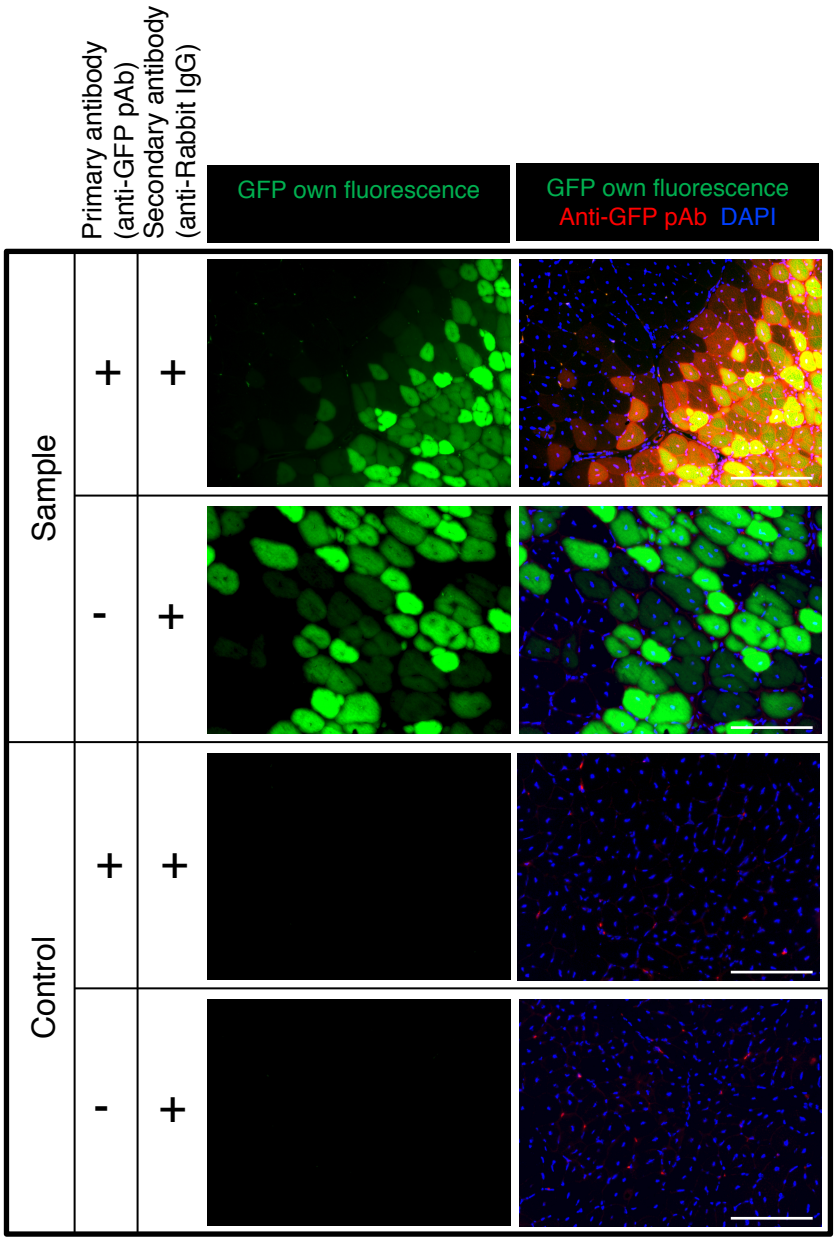

Figure S5. Detection of GFP-positive myofibres from TA muscles transplanted with GFP positive satellite cells. The specificity of GFP-positive myofibres was confirmed by immunostaining with an anti-GFP antibody (red). Scale bar represents 200 μm.

Figure S6

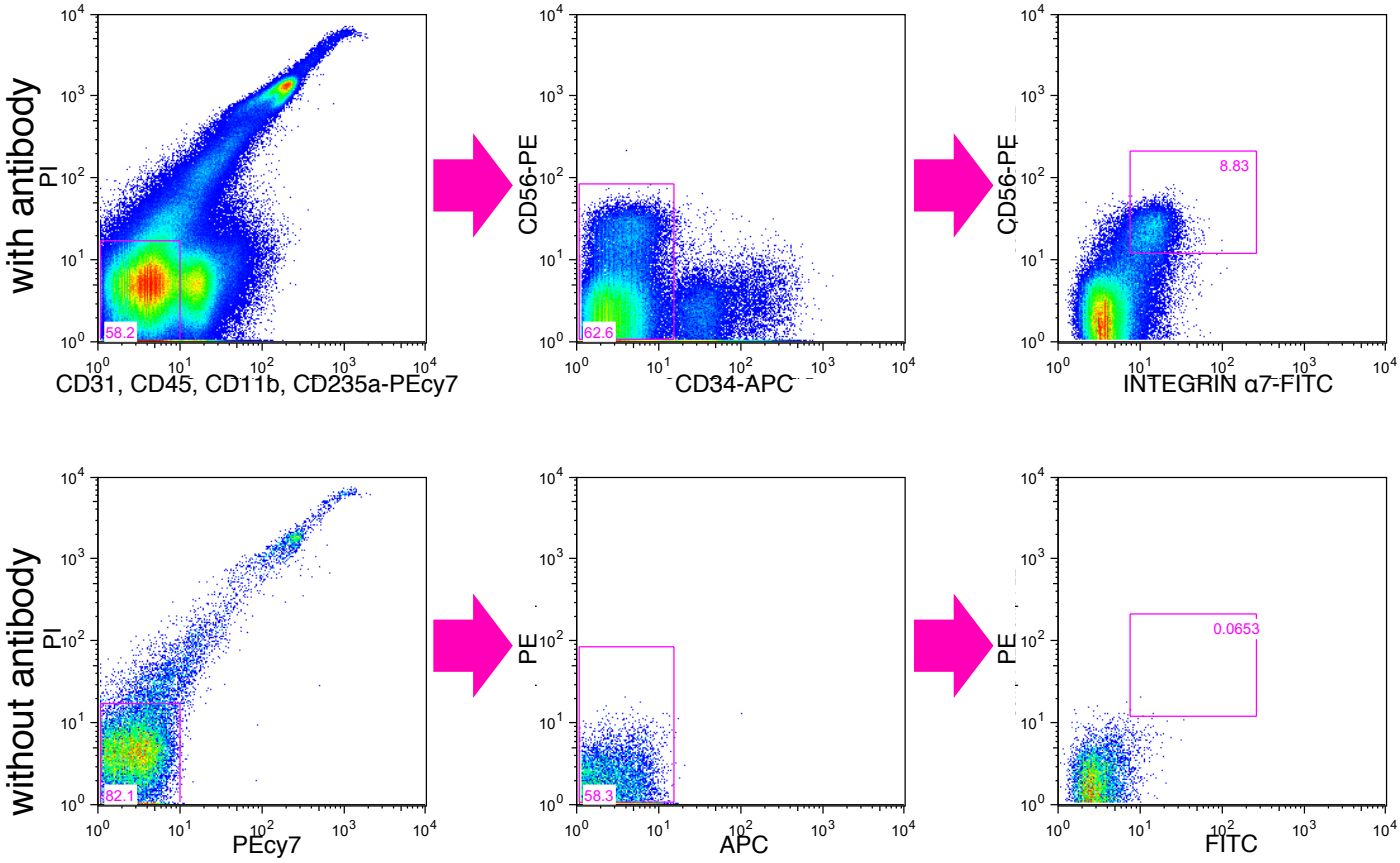

Figure S6. FACS profiles of satellite cells from human.
The CD31−CD45−CD11b−CD235a−CD34−CD56+INTEGRIN α7+ cells were analyzed as human muscle satellite cells using the MoFlo.

Figure S7

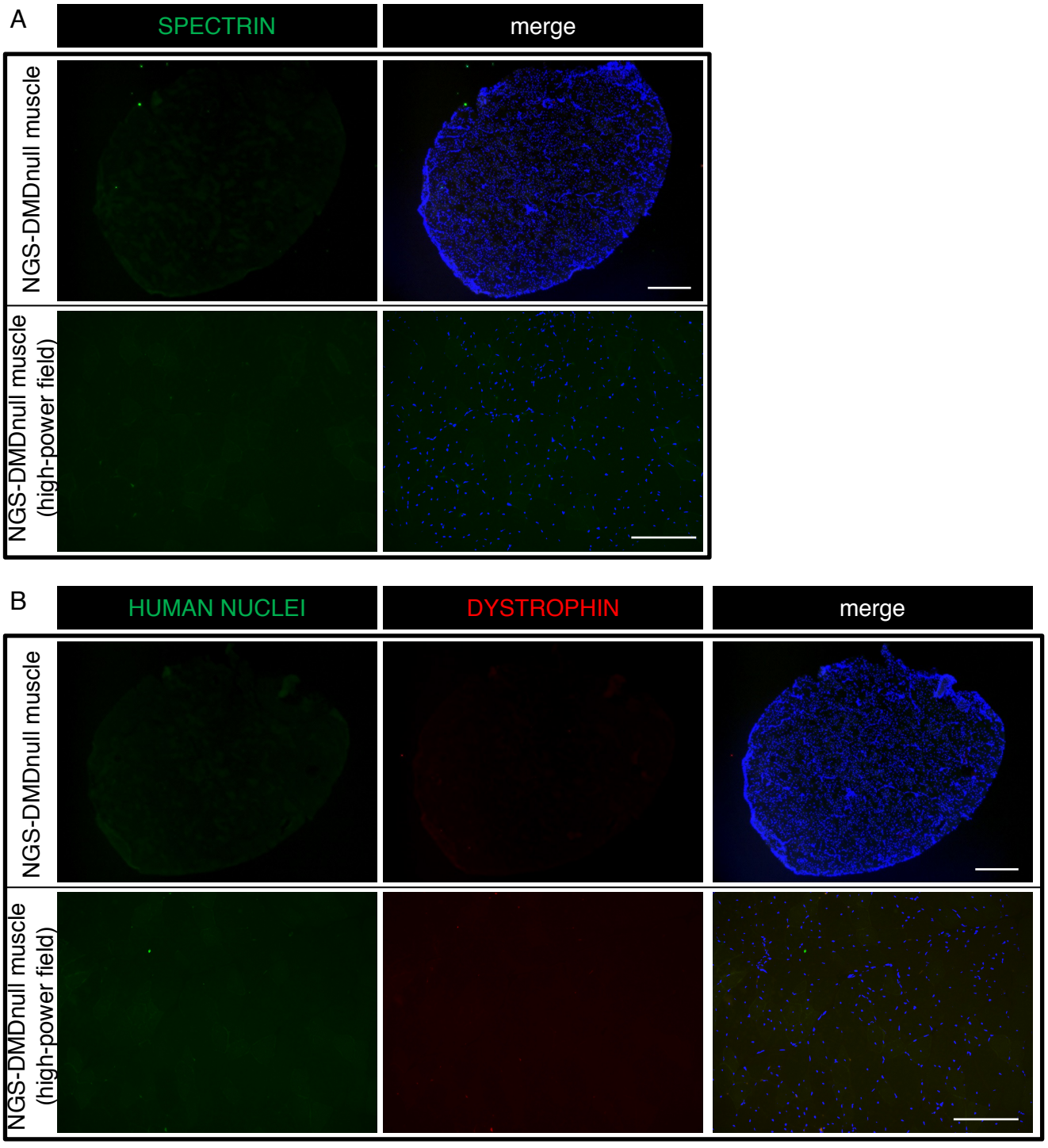

Figure S7. Immunostaining of TA muscle of NSG-DMDnull mice. (A) Immunostaining of cross-section of the contra lateral TA muscle of NSG-DMDnull mice for HUMAN SPECTRIN antibody (green) and DAPI (blue). (B) Immunostaining of cross-section of the contra lateral TA muscle of NSG-DMDnull mice for DYSTROPHYN antibody (red) and HUMAN NUCLEI antibody (green) and DAPI (blue). Scale bar represents 500 μm (upper figures) and 200 μm (lower figures).

SUPPLEMENTAL EXPERIMENTAL PROCEDURES

Mouse and human samples

C57BL/6 wild-type mice and C57BL/6-Tg (CAG-EGFP) mice were purchased from CLEA Japan, Inc. and Japan SLC, Inc., respectively. Eight to twelve-week-old male mice were analyzed. All procedures for animal experiments were approved by the Tokyo Medical and Dental University Animal Care and Use Committee (Protocol number: 0170282C). Human samples were obtained from semitendinosus muscle from patients undergoing anterior cruciate ligament reconstruction at Tokyo Medical and Dental University Hospital. All experiments were approved by the local Institutional Review Board of Tokyo Medical and Dental University (No. 2121) and all study participants provided written informed consent. NSG mice were purchase from Charles River Japan, Inc. DMD-null/NSG mice were generated by mating DMD-null/NODscid mice (Tanaka et al., 2013) and NSG mice in the Animal Facility of Center for iPS Cell Research and Application (CiRA), Kyoto University. Some animal experiments were carried out in the Animal Facility of CiRA following protocols approved by the Animal Research Committee of Kyoto University (No.10-1-11) and by the Ethics Committee of the Graduate School of Medicine, Kyoto University and the Kyoto University Hospital (No. 57).

Muscle injury model

Mice were anesthetized with isoflurane, and hairs in their hind limbs were shaved. One hundred microliters of CTX (10 μM in 0.9% NaCl; Sigma-Aldrich) was injected into the tibialis anterior (TA) muscle using a 29-gauge needle. Seven or 14 days after injections, mice were euthanized and the frozen tissue sections were prepared for analysis as described above.

Cryosectioning

Mouse TA muscle and human semitendinosus muscle were dissected out and frozen in liquid nitrogen-cooled isopentane (Wako). Using a cryostat (Leica), the frozen TA muscles were sectioned transversely at a thickness of 8 μm, and sections from the widest part of the muscle were attached to MAS-coated slide glasses (MATSUNAMI). Cryosections were kept at −80°C until used for immunostaining.

Immunofluorescence

The cryosections described above were used for immunohistochemistry. Primary satellite cells were cultured on 8-well chamber slides (MATSUNAMI) coated with Matrigel (BD Biosciences) or laminin-E8 fragment. Tissue sections or cells were fixed in 4% paraformaldehyde in PBS for 10 minutes at room temperature, and then permeabilized with 0.2% Triton X-100 (Sigma-Aldrich) in phosphate-buffered saline

(PBS) for 15 minutes at room temperature. After blocking with Power Block Universal Blocking Reagent (BioGenex) or M.O.M. kit (Vector Laboratories), the fixed cells were incubated with primary antibodies overnight at 4°C. After washing, bound primary antibodies were labeled with fluorescence-conjugated secondary antibodies for one hour at room temperature. The immunostained samples were mounted with mounting medium for fluorescence with DAPI (Vector Laboratories). Primary and secondary antibodies were as follows: anti-LAMININ α2 (Sigma-Aldrich, L0663), anti-PAX7 (SantaCruz, sc-81648), anti-KI67 (Leica, NCL-Ki67p), anti-MYOD (SantaCruz, sc-760), anti-pJNK (Cell Signaling, 9251S), anti-p-p38 (Cell Signaling, 9211S), anti-HUMAN NUCLEI (Millipore, MAB1281), anti-SPECTRIN (Leica, NCL-SPEC1), anti-DYSTROPHIN (Abcam, ab15277) and mouse/rabbit/rat IgG-Alexa488, -Alexa594, or Alexa647 (Life Technologies). Fluorescent images were obtained using a BZ-X710 (Keyence) and a LSM700 laser scanning confocal microscope (ZEISS). Fluorescence intensity was quantified by automated image analysis using the BZ-X analysis software (Keyence).

Flow cytometry

Skeletal muscle samples from mouse fore- and hind-limbs and human semitendinosus muscle were dissected out and digested with 0.14% collagenase type II (Worthington Biochemical) for one hour at 37°C. Then, the digested tissue was filtered through 100 μm- and 40 μm-cell strainers (BD Biosciences). The

filtered mononuclear cells were stained with phycoerythrin (PE)-conjugated anti-CD31 (BD Biosciences, 553373), PE-conjugated anti-CD45 (BD Biosciences, 552848), PE-conjugated anti-SCA1 (BD Biosciences, 553335), and biotinylated anti-SM/C-2.6 antibodies and streptavidin-allophycocyanin (APC) (Becton, Dickinson and Company, 555516). In human: PEcy7-conjugated anti-CD31 (BD Biosciences, 563651), PEcy7-conjugated anti-CD45 (BD Biosciences, 557748), PEcy7-conjugated anti-CD11b (BD Biosciences, 557743), PEcy7-conjugated anti-CD235a (BD Biosciences, 563666), APC-conjugated anti-CD34 (BD Biosciences, 555824), PE-conjugated anti-CD56 (BD Biosciences, 555516) and INTEGRIN α7 Antibody (3C12) [FITC] (Novus Biologicals, NBP1-54412) on ice for 30 minutes. Cell sorting was performed using a MoFlo flow cytometer (Beckman), and $CD31^{-}$, $CD45^{-}$, $SCA\text{-}1^{-}$, and $SM/C\text{-}2.6^{+}$ cells were collected as mouse satellite cells, and $CD31^{-}$, $CD45^{-}$, $CD11b^{-}$, $CD235a^{-}$, $CD34^{-}$, $CD56^{+}$, INTEGRIN $\alpha7^{+}$ cells were collected as human satellite cells.

Phosphorylated signal analysis

For intracellular staining of phosphorylated JNK, ERK, FAK, p38 MAPK, p130CAS, STAT3, SRC, AKT and p53, stimulated cells were fixed with fixation buffer (BD bioscience) for 15 min at 37°C, and then permeabilized with perm wash buffer (BD bioscience) for 25 min at 37°C. Cells were incubated with PE

Mouse anti-JNK (pT183/pY185) (BD Bioscience, 562480), PE Mouse anti-ERK1/2 (pT202/pY204) (BD Bioscience, 612566), PE Mouse anti FAK (pS910) (BD Bioscience, 558450), PE Mouse anti-p38 MAPK (pT180/pY182) (BD Bioscience, 612565), PE Mouse anti-p130CAS (pY249) (BD Bioscience, 558538), PE Mouse anti-STAT3 (pY705) (BD Bioscience, 612569), PE Mouse anti-SRC (BD Bioscience, 560094), Alexa Fluor 488 Mouse anti-Akt (pS473) (BD Bioscience, 560404) and Alexa Fluor 488 Mouse anti-p53 (pS37) (BD Bioscience, 560282). Phospho-flow analysis was performed using an Aria flow cytometer (BD Bioscience).

RT-PCR

Total RNA was isolated from sorted cells and primary myogenic culture using TRY reagent (Sigma-Aldrich). cDNA was generated from 0.5 µg total RNA using SuperScript III First- Strand Synthesis SuperMix for qRT-PCR (Invitrogen), previously treated with DNAse. RT-PCR was performed using Applied Biosystems Step One Real Time PCR System. PCR was performed in duplicate with reaction volumes of 10 µl, containing Fast SYBER Green Master Mix (Applied Biosystems), forward and reverse primers and cDNA template. Data were analyzed using a comparative critical threshold (Ct) method where the amount of target normalized to the amount of endogenous control reactive to control value is given by

$2^{-\Delta\Delta Ct}$. We used following primers: *HPRT*: 5′-tcagtcaacggggacataaa-3′ (forward), 5′-ggggctgtactgcyyaaccag-3′ (reverse), *Pax7*: 5′-ctcagtgagttcgattagccg-3′ (forward), 5′-agacggttccctttgt-3′ (reverse), *Myogenin*: 5′-gaaatgaatgaggccttcg-3′ (forward), 5′-caaatgatctcctgggttgg-3′ (reverse).

Statistical analysis

Sample sizes, replicate numbers, and p-values are stated in the figure legends. Three or more animals were used per experiment. Biological replicates were tested with individual mouse and human samples. Sample sizes were not based on power calculations. No animals used for the experiments were excluded from analyses. Results were shown as means ± standard deviations or standard errors of the mean, depending on the size of the samples. *P* values are indicated either with the number on the graphs or with asterisks: **P*<0.05, ***P*<0.01, and ****P*<0.001. Differences between groups were assessed by using the Student's two-tailed t test for independent samples. Differences among more than two groups were analyzed using one-way ANOVA followed by Tukey-Kramer post-hoc tests. Values of *P*<0.05 were considered statistically significant. All data are means ± SEM.